الجـــمـــهـــوريـــــــةالجـــ
ـــزائــريـــة الديمـــقــراطـيـــة
الــشـــعــبـيـــة

People’s Democratic Republic of Algeria وزارة
التـــعـــليـــم العـــالي و
البـــحث العـــلـــمـــي

Ministry of Higher Education and Scientific Research

جـــامعة أبي بـكـــر بـلــقـــايـد –
تـــلمســـان –

University Abou bakr Belkaïd– Tlemcen –
Faculty of TECHNOLOGY

THESIS

Presented for obtaining a Master’s degree in Civil engineering

Speciality: Structural engineering

By: Chifumuro Taniah Smoke

TITLE

Seismic Behaviour and Shear Capacity of Reinforced Concrete Short Coupling Beams

Thesis defended on : 06 /06 /2024, before the jury composed of :

Pr Abdellatif MEGNOUNIF	University of Tlemcen	President
Mm Medjahed Amina	University of Tlemcen	Examiner
Pr Mohammed MATALLAH	University of Tlemcen	Ssupervisor
Dr Nadia HAMIMED	University of Tlemcen	Co-Supervisor
Dr Ahmed BELBACHIR	University of Tlemcen	Co-Supervisor

Academic Year :
2023/2024

Acknowledgements

Foremost, I want to offer this endeavour to God Almighty for the wisdom, strength, peace of mind and good health to complete this research. I am deeply grateful to Jesus Christ, the amazing grace He brought, this grace that has carried me this far and for the Holy Spirit for always being with me.

Secondly, I want to express my sincere gratitude to my research committee. To Professor Mohammed MATALLAH for proposing the topic and for bringing the weight of your considerable experience and knowledge, your high standard has made me better at what I do. I also want to acknowledge Dr Ahmed BELBACHIR who provided invaluable guidance on the Cast3m software, this project was a success because of his effortless support. I am deeply indebted to Dr Nadia HAMIMED for her utmost counsel in the writing of this research; her corrections and patience were of great value to me.

To my family, my father, Mr T.J Chifumuro, thank you for always being there for me, your unconditional love, and your financial support made it possible for me to complete this project and in all the years of my university studies. To my loving mother, thank you for all the sacrifices you made for me to be here. To my siblings, thank you all, for your motivation and support, the journey was easier because of you. In addition, to my friends who now have become family, I treasure your support, good wishes, and prayers.

Finally yet importantly, I would like to thank the University of Tlemcen in Algeria for granting me this opportunity to study and to be trained as an up-coming engineer, without this opportunity, this project would not have begun. My joy knows no bounds in expressing my cordial gratitude.

Taniah Smoke Chifumuro

Table of Contents

List of Figures v

List of Symbols viii

List of Abbreviations x

Abstract xi

General Introduction 12

1.1 Introduction 14

1.2 What are Coupling Beams 14

1.2.1 Span-to-Depth Ratio (Lnh) 22

1.2.2 Shear Stress (V) 23

1.2.3 Reinforcement Details 23

1.2.4 Anchorage of Beam Flexural Reinforcement 23

1.3 International Standard Codes Provisions 23

1.3.1 Algerian Seismic Rules RPA99/Version2003 23

1.3.2 Euro Code 8 (EC8) 25

1.3.2 ACI 318-14 Building Code 27

1.3.3 ACI 318-19 30

1.3.4 ASCE-41-17 (American Society of Civil Engineers) 32

1.3.5 IS13920 (2016) - (Indian Standard Institution) 35

1.4 Advanced Methods 35

1.4.1. The Strut and Tie Method (STM) 35

1.4.1.2 Equilibrium Condition 40

1.4.2 The Compatibility Stress Field Method (CSFM 42

1.5 Conclusion 45

Chapter 2: Previous Experimental Studies On Coupling Beams 46

2.1 Introduction 46

2.2 Motives behind the Experimental Studies 46

2.3 Testing Variables Used to Analyse Coupling Beams in Previous Experimental Studies 47

2.3.1 Reinforcement Configuration 48

2.3.2 Conventionally Reinforced Coupling Beams (CRCBs) 48

2.3.3 Diagonally Reinforced Coupling Beams (DRCBs) 52

2.4 Different Reinforcement Configurations 56

2.5 Conclusion 59

CHAPTER 4: Numerical Analysis of Diagonally Reinforced Short Coupling Beam 74
4.1 Introduction..74
4.2 Numerical Modelling of the DRCB-FC specimen using Cast3m...............................74
4.3 Crack operation of the DRCB-FC specimen 76
4.4 DRCB-FC's Load-Displacement Curves 77
4.5 Shear Strength Analysis 79
4.6 Conclusion 80
General Conclusion...84
References...85

List of Figures

....14

Figure 1.1: Coupled and Coupling Beams (Courtesy to Taranath 2010) 14
Figure 1.2: A coupled shear wall system. 15
Figure 1.3: The coupled shear wall core of a multi-storey building in the Seattle area. (Cary Kopczynski&Co.Bellevue, WA). 15
Figure 1.4: Formation of plastic hinges in short coupling beams due to lateral loads 17
Figure 1.5: (a) isolated wall and (b) coupled wall 17
Figure 1.6: High-rise building (30 plus storey-building) with short coupling beams (courtesy to www.alarmy.com). 18
Figure 1.7: (a) CRCBs and (b) DRCBs 19
Figure 1.8: Standard reinforcement detailing in earthquake-resistant coupling beams...........20
(Courtesy to RémyLequesne). 20
Figure 1.1.1: Plastic deformations on (a) solid wall and (b) coupled wall system (courtesy to Emre TOPRAK et al)..21
Figure 1.1.2 : (a) Relationships between wall and coupling beam rotations; (b) strain of horizontal top chord of coupling beams (Jang & Hong, n.d.)..22
Figure 1.1.3: Sail cut in elevation (courtesy to RPA99V2003). 24
Figure 1.1.4: Lintel (coupling beam) reinforcement (RPA99/V2003) 25
Figure 1.1.5: Forces in the lintel connecting rods (RPA99/V2003). 25
Figure 1.1.6: Coupling beams with diagonal reinforcement (Euro Code 8)............................27
Figure 1.1.7: Wall with an opening (ACI 318-14)..28
Figure 1.1.8: Confinement of individual diagonals of DRCB (ACI 318-14). 29
Figure 1.1.9: Full confinement of diagonally reinforced concrete beam section 30
Figure 1.1.10: Wall with an opening (ACI 318-19)..30
Figure 1.1.11: Diagonal reinforced coupling beam (ACI 318-19). 31
Figure 1.1.12: RCC coupling beam design as per ACI..32
Figure 1.1.13: Effective stiffness value of coupling beams (ASCE-41-7) 33
Figure 1.1.14: Plastic hinge rotation in the shear wall, where flexure dominates inelastic response (ASCE-41-17). 33
Figure 1.1.15 :**(a)** Story Drift in a Structural Wall with Inelastic Response Predominating Shear 34
(b) Chord rotation for structural wall coupling beams (ASCE-41-17)...................................34
Figure 1.1.16: Description of strut and tie method (ACI 318-19) 36
Figure 1.1.17: Description of strut-and-tie model (ACI 318-14)..37
Figure 1.1.18: (a) and (b) D-Regions and discontinuities (courtesy to ACI 318-19). 38
Figure 1.1.19: Resolution of forces on a nodal zone (courtesy to ACI 318-19)......................39
Figure 1.1.20: (a) truss action, (b) arch action, (c) strut-and-tie model, and (d) tensile force of the top steel. 41
Figure 1.1.21: (a) displacement by truss action; (b) displacement by arch action; (c) displacement by flexural rotation; (d) top chord strain and (e) displacement by beam elongation...42
Figure1.1.22 :Discontinuity regions (Navrátil et al., 2017)..43
Figure 1.1.23 : Principal stresses in concrete and reinforcement (Mata Falcón et al., 2022)..44
Figure 2.1: conventionally reinforced coupling beam. 48
Figure 2.2: A typical load-rotation curve observed by Paulay (1974) for CRCBs with aspect ratio of 1.29..49

Figure 2.3: Distortions associated with the elongation of the top and bottom flexural bars of the conventionally reinforced coupling beams (Santhakumar). 50
Figure 2.4: Sliding shear failure in coupling beams (courtesy to Park and Paulay 1975). 51
Figure 2.5 : Diagonally reinforced coupling beam (Monthian Setkit, 2012)...........................53
....53
Figure 2.6: Professor Tom Paulay working on the Diagonally reinforced coupling beam in the core wall of Christ church General Hospital (courtesy of J.I.Restrepo). 53
Figure 2.7: Mechanism of load resistance in a diagonally reinforced coupling beam (Paulay and Santhakumar 1976). 54
Figure 2.8: Coupling beam reinforcement configuration with diagonal bars at the locations of plastic hinges (Monthian Setkit, 2012). 57
Figure 2.9 :Reinforcement configurations investigated by Tassios (Monthian Setkit, 2012) .58
Fig.3.1 Phase-by-phase displacement-regulated cyclic loading trajectory (Sesli & Husem, 2021). 61
Figure 3.2: Dimensions and reinforcement details of Conventionally reinforced coupling beam specimen: (CRCB)(Sesli & Husem, 2021). 62
Fig.3.3: Mesh of the Finite-Element Model of CRCB...64
Fig.3.4: Benchmark Model of CRCB under Cyclic Loading. 64
Fig.3.5: Failure mode of CRCB under static loading. 65
Fig.3.6: Failure mode of CRCB under quasi-cyclic loading. 66
Fig.3.7: (**a**)The condition of experimental CRCB specimen after failure (Sesli & Husem, 2021); (**b**)The condition of numerical CRCB model after failure. 67
Fig.3.8: Load-displacement curve of CRCB specimen under static loading. 68
Fig.3.9: Numerical and Experimental bilinear curves for CRCB 68
Fig.3.10: Load-displacement curve of CRCB under cyclic loading (Sesli&Husem, 2021). ...69
Fig.3.11: CRCB Load-displacement envelope. 69
Fig.3.12: An analogous elasto-plastic system that was employed to standardise the energy dissipated per cycle. 70
Fig.3.13 CRCB Shear strength results 72
Fig.3.14: Definition of ductility on load-displacement envelope curve. 73
Fig.4.1: Benchmark model of DRCB-FC ....**Erreur ! Signet non défini.**
Fig.4.2: Cast3m DRCB-FC specimen..75
Fig.4.3: Experimental specimen of Diagonal reinforcement with full confined section (DRCB-FC). 75
Fig.4.4: DRCB-FC cracking mechanism under static loading. 77
Fig.4.5: DRCB-FC cracking mechanism under quasi-static cyclic loading. 77
Fig.4.6: Load-displacement relationship of DRCB-FC specimen. 78
Fig.4.7 DRCB-FC Envelope curve. 78
Fig.4.8: DRCB-FC Bilinear response curve. 79
Fig.4.9: DRCB-FC shear strength...80
Fig.5.1: (a) CRCB and DRCB-FC under quasi-static cyclic loading**.** 81
Fig.5.2: DRCB-FC and CRCB Numerical Shear Strength results. 81
Fig.5.3 DRCB-FC and CRCB bilinear pushover curves. 82
Fig.5.6: Ductility results for CRCB and DRCB-FC specimens...82

LIST OF TABLES

Table 1: Conventionally Reinforced Short Coupling Beam Specimen-Geometry 63
Table 2: Spacing, Concrete and Steel Strength of Conventionally Reinforced Short Coupling Beam specimen 63
Table 3.1: Shear Strength results 71
Table.3.2: Theoretical Shear Strength 71
Table 3.3: Summary of CRCB Results 73
Table 4.1: DRCB-FC specimen Geometry 75
Table 4.2: DRCB-FC specimen concrete and steel properties 76
Table 4.3: DRCB-FC drift ratio and ductility 79
Table 4.4: Shear Strength Results for the DRCB-FC 79
Table 4.5: Theoretical Shear Strength for DRCB-FC 80

List of Symbols

$\sqrt{f'c}$ – shear strength

bo - thickness of the lintel

h- beam depth

Ln- clear span

AD- diagonal reinforcement cross-sectional area

VEd – design shear force

fctd – design value of the tensile strength of concrete

bwd – the thickness of the boundary element in the web

α – the angle between the beam’s axis and the diagonal bars

Asi – total area of steel bars in each diagonal direction

At- steel in the current part

Av – area of vertical reinforcement in coupling beam

bw – web width of the coupling beam

bwd – thickness of the boundary element in the web

C – Compression zone

C1 – truss mechanism’s diagonal strut

C1, C2- centroid of the walls

C2 – diagonal strut

Cu – compression reinforcement

d - Useful height

dw - length of the wall

E – Young’s modulus of elasticity

EA – Axial rigidity

EI – Flexural rigidity

fce – effective compressive strength

fctd – design value of the tensile strength of concrete

Fnn – nominal strength at face of a nodal zone

Fnt – nominal strength

Fus – factored compressive strength

fyd – design value of yield strength concrete

fyv – yield strength of the vertical reinforcement in coupling beam

fyw – stirrups yield strength

h - beam depth

Ln, av - clear span

lp – assumed plastic hinge

MyE – moment strength at section

n – modular ratio

Tu - diagonal reinforcement

VEd – design shear force

Vj – nominal joint shear strength

Vn – calculated nominal shear strength

α – the angle between the beam's axis and the diagonal bars

αc – coefficient of concrete strength

Δtl – horizontal displacement of the left portion of coupling beam

Δtr – horizontal displacement of the right portion

θwd - rotation capacity of walls

θy – yield point

λ – modification factor

λs – factor used to modify shear strength

ρ – ratio of gross concrete are

ρl – ratio of longitudinal reinforcement

ρt – ratio of transverse reinforcement

φ – strength reduction factor

φn - strength reduction factor

βc – confinement modification factor for struts

βs – factor used to account for the effect of cracking

List of Abbreviations

ACI – American Concrete Institute

CEA – Atomic Energy Commission

CRCCBs- conventionally reinforced concrete coupling beam

CSFM – Compatible Stress Field Method

CSW- coupled shear wall

CWs – coupled wall systems

DRCCB - diagonally reinforced concrete coupling beam

DRCCB-FC – Diagonally Reinforced Concrete Coupling Beam Full Confined concrete section

D-regions – Discontinuity regions

EC8 – Euro code 8
FEMA – Federal Emergency Management Agency
HPFRC – High Performance Fibre Reinforced Concrete
M, V- Moment/Shear respectively
RC - reinforced concrete
STM – Strut-Tie-Model

Abstract

In reinforced concrete buildings, short coupling beams located above openings (windows, doors or elsewhere …) are generally used to join shear wall segments together in order to transfer and resist the lateral loads from earthquake or wind actions. Two **types of reinforcing SCB beam are used: Conventional Reinforced Concrete Coupling Beams (CRCCB) and diagonally reinforced concrete coupling beams (DRCCB).** Coupling beams should exhibit excellent energy dissipation capacity; however, **because of their complexes behavior their design is often inappropriate.**

The present study is an advancement of the efforts aiming to investigate the behavior of the SCB (both CRCCB and DRCCB) in order to understand the dissipation mechanisms during the failure process.

Key words: RC structures, Short coupling beams, numerical modelling, dissipations.

<u>Résumé</u>

Les poutres de couplage courtes (situées au-dessus des ouvertures …) sont généralement utilisées pour assembler les segments de murs de cisaillement afin de transférer et de résister aux charges latérales dues aux séismes ou aux vents. Deux types de poutres courtes sont utilisés : les poutres de couplage en béton armé conventionnelles (CRCCB) et les poutres de couplage en armé diagonalement (DRCCB). Les poutres de couplage doivent assurer une excellente capacité de dissipation d'énergie, cependant, en raison de leur comportement complexe, leur conception est souvent inappropriée.

La présente étude constitue une avancée dans les efforts visant à étudier le comportement des poutres courtes (CRCCB et DRCCB) afin de comprendre les mécanismes de dissipation lors de leur rupture.

Mots clefs : Structures en béton armé, poutres de couplage courtes, modélisation numérique, dissipations.

ملخص

في المباني الخرسانية المسلحة، يتم استخدام عوارض التوصيل القصيرة الموجودة فوق الفتحات (النوافذ أو الأبواب أو أي مكان آخر...) بشكل عام لربط أجزاء جدار القص معًا من أجل نقل ومقاومة الأحمال الجانبية الناتجة عن الزلازل أو الرياح. يتم استخدام نوعين من عوارض SCB المعززة: عوارض التوصيل الخرسانية المسلحة التقليدية (CRCCB) وعوارض التوصيل الخرسانية المسلحة قطريًا (DRCCB). يجب أن تظهر عوارض التوصيل القصيرة قدرة ممتازة على تبديد الطاقة، ومع ذلك، نظرًا لسلوكهم المعقد ، فإن تصميمها غالبًا ما يكون غير مناسب. تعد الدراسة الحالية بمثابة خطوة للجهود الرامية إلى دراسة سلوك SCP (CRCCB وDRCCB) من أجل فهم آليات تبديد الطاقة أثناء الانهيار

الكلمات الدالة
الهياكل الخرسانية المسلحة، عوارض التوصيل القصيرة ، النمذجة الرقمية، آليات تبديد الطاقة.

General Introduction

In the design of mid-to high-rise buildings, controlling the lateral displacements of a structure subjected to seismic loads is a major concern. Since coupling beams couple the actions of structural walls to create an effective lateral load-resisting system, they have a significant impact on the behaviour of coupled wall systems (CWSs). Determining how reinforcement layouts affect the behaviour of structural elements may make significant contributions to the construction field. For short-reinforced coupling beams, precise reinforcement detailing is necessary to guarantee appropriate coupling beam behaviour under stresses and deformations brought on by earthquake actions, usually, in the shape of wide confinement reinforcement and diagonal bars. By distributing inelastic deformation between the coupling beams and wall piers both vertically and in plan, coupled walls are an excellent technique for resisting lateral loads. Due to transport facilities, doors, windows, and other openings connected by coupling beams, the majority of reinforced concrete (RC) shear walls have openings (D-regions). Examining coupled shear wall performance is necessary to ensure the stability and security of tall structures in the event of an earthquake. An adequate global response can only be achieved when coupled shear walls are used in the seismic design of buildings if the coupling beams respond in a ductile mode. Shear walls joined by coupling beams (coupled shear walls) function as a single structure and are more effective at withstanding lateral loads than separate shear walls without coupling beams (isolated walls).

According to the beam theory, where the length-to-depth ratio is greater than two, the Bernoulli Navier hypothesis of plane strength is valid for classical calculations and it is valid and executed according to the Euro code. In contrast, short coupling beams have a length-depth ratio that is less than or equal to two and have discontinuity regions (D-regions) where the Bernoulli Navier hypothesis is not valid, therefore, there is a need for the use of advanced methods. This study reviewed the current difficulties in seismic design for short coupling beams using international standard codes and bridged the gap found in these codes with advanced methods to provide adequate shear failure resistance under lateral loads. Assuming that they would sustain all shears, the number of diagonal bars in the existing design specifications is correspondingly calculated, resulting in a high degree of reinforcement. To create a new design with better seismic performance, a new design for coupling beams was developed through extensive research on their seismic behaviour in the 1970s (Monthian Setkit, 2012). Diagonal reinforcement has been widely accepted in seismic design worldwide because experimental studies (Luciano Galano and Andrea Vignoli, 2000; Paulay, 2011) have demonstrated that it significantly improves ductility, stiffness retention, and energy dissipation in short coupling beams (SCBs). However, there are meticulous construction issues with the diagonal reinforcement details. Reports show that reinforced diagonals are effective when the beam has a span-to-depth ratio of less than two. However, span-to-depth ratios for modern buildings are usually between 2.4 and 4, which when combined with the detailing requirements, results in an extremely shallow angle of inclination which is less than twenty degrees (Monthian Setkit, 2012). There is doubt about diagonal reinforcement's efficacy.Reviewing the seismic behaviour of short coupling beams under lateral (shock) stresses was the aim of this study. The priority was to analyse the risk of shear failure in short reinforced coupling beams during lateral load actions and to provide designing ways that can provide adequate time to protect the integrity of human lives. Additionally, the main concern was to appraise the reinforcement layouts avowed in the international standard codes and their contribution in the behaviour of coupling beams. To validate this, experimental results were compared with the numerical results under quasi-static cyclic dynamic loads, using equations provided in the codes and to forecast linked shear walls' shear strength under the influence of lateral loads.

There are four chapters in this research study. Firstly, in chapter one, there is a literature review of previous work related to this study. Secondly, the second chapter concentrated on the experimental research done by scientists in the past, on the behaviour of SCBs. Analytical work from the tests of conventionally reinforced coupling beam (CRCB) specimen, were evaluated using numerical analysis, later discussed in the third chapter. Chapter 4 focused on the finite element modelling of the diagonally reinforced short coupling beam (DRCB) specimen. My work ended with the general conclusion.

Chapter 1: Literature Review on Coupling Beams

1.1 Introduction

This chapter presents an overview of topics related to this research study and background information on coupling beams. A review of formulas given by international standard codes is presented in Section 1.3, of particular interest is the design of CRCBs and DRCBs. Following, Section 1.4 which provided formulas used by advanced methods, namely the strut and tie model method (STM) and the compatible stress field method (CSFM). In Section 1.5, there is the conclusion for the chapter.

1.2 What are Coupling Beams

In order to provide an effective lateral load resisting system and to reduce the total seismic demand for coupled structural shear walls, coupling beams are utilized to couple the actions of the walls. An effective lateral load-resisting system is created by coupling the actions of structural walls with coupling beams (Fortney et al., 2006). They must thus have sufficient energy dissipation capacity and be able to withstand significant inelastic deformations. The coupled wall system lowers the deformation demands on structures (see Fig. 1.1).

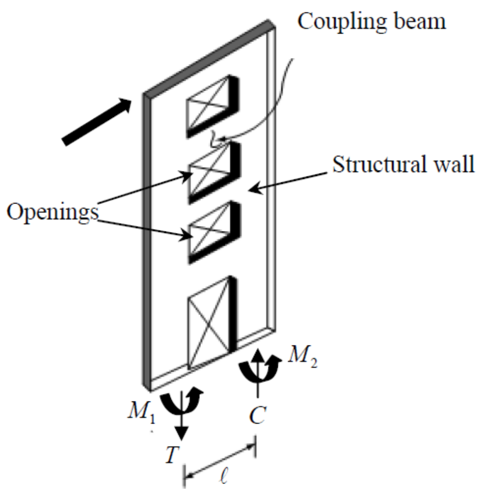

FIGURE 0: COUPLED AND COUPLING BEAMS (TARANATH 2010)

Chapter 1: Literature Review on Coupling Beams

The behaviour of coupling beams significantly influences the structural behaviour of reinforced concrete coupled walls (Figs. 1.2 and Fig. 1.3).

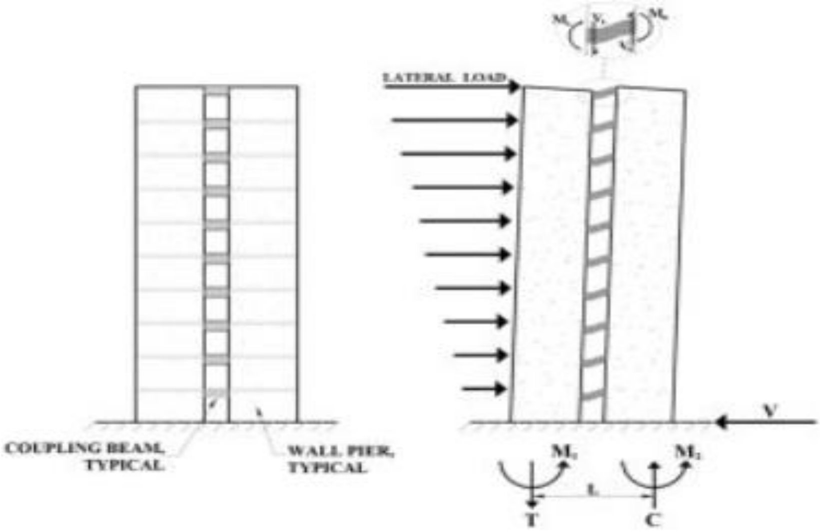

FIGURE 1.2: A SYSTEM OF COUPLED SHEAR WALLS

FIGURE 1.3: THE COUPLED SHEAR WALL CORE OF A MULTI-STOREY BUILDING (CARY KOPCZYNSKI&CO.BELLEVUE, WA).

Coupling beams must be designed for both flexural and shear resistance. Therefore, they are termed 'coupled beams' when they can take the load of the walls; otherwise, they will show failure and cannot be designed as normal beams. Short coupling beams have to give way in front of the wall piers, operate in a ductile manner, and have notable energy-absorbing qualities (dissipation). Nonetheless, reinforced short concrete coupling beams are exceedingly challenging to build in contemporary practice (Monthian Setkit, 2012).

In seismic design, there are many influencing factors on structural types, such as soil conditions, general economic considerations, availability, cost of main structural materials, legal factors (zoning and codes) etc. (Macdonald, 1997). Some materials exhibit multiple cracks under uniaxial tension, however, due to improvements in concrete technology, structural applications of strain-hardening or high-performance fibre-reinforced concrete (HPFRC) have been experimentally investigated (Fantilli et al., 2009). Test results (Gustavo J. Parra-Montesinos, 2005) have shown that HPFRC is a viable alternative to regular concrete in shear critical members. Additionally, (Fantilli et al., 2009) test results have shown that the use of HPFRC in short coupling beams (SCBs) can successfully eliminate the problem of reinforcement congestion without compromising seismic performance. Large-scale test results further demonstrated the better stiffness retention capacity and damage tolerance of HPFRC coupling beams with short and intermediate aspect ratios (Monthian Setkit, 2012).

Previous experimental findings have demonstrated that short coupling beams constructed as traditional reinforced concrete beams (CRCBs), which, because of their very small span-to-depth ratio and solely longitudinal and transverse steel reinforcement, typically exhibit brittle shear and slide failure (Monthian Setkit, 2012). Well-proportioned coupling beams generally develop plastic hinges above the building's height (see Fig. 1.4), resulting in good energy dissipation (Aktan & Bertero, 1981).

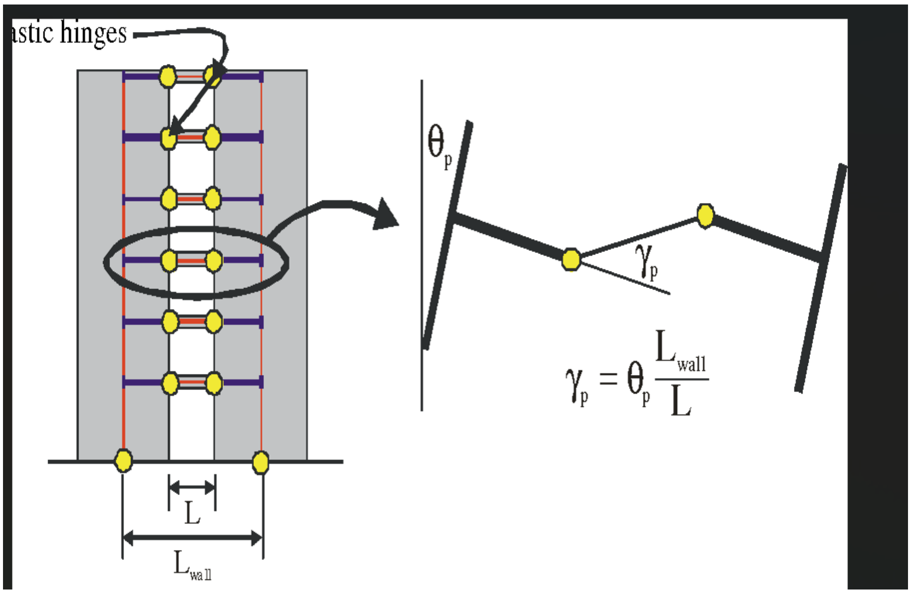

FIGURE 1.4: PLASTIC HINGE FORMATION DUE TO LATERAL LOADS IN SHORT COUPLING BEAMS

Coupled wall systems are more efficient than isolated walls because the walls are coupled generate more lateral strength, stiffness, and strength (Fig. 1.5).

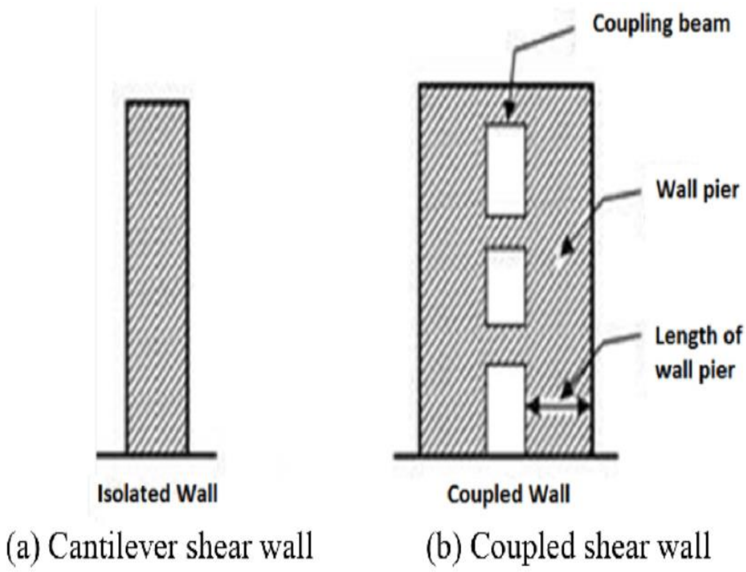

FIGURE 1.5: (A) ISOLATED WALL AND (B) COUPLED WALL

Chapter 1: Literature Review on Coupling Beams

Prior research findings have indicated the importance of diagonal reinforcement in coupling beams and the ways in which short coupling beams behave differently from regular beams (T.Paulay, 1969). Furthermore, a great deal of research has been done on reinforced concrete (RC) coupling beams (Monthian Setkit, 2012). Constrained diagonal reinforcement offered superior shear resistance and ductility in deep coupling beams, as shown by previous scientists (Paulay, 2011). Diagonal reinforcement has emerged as the cutting-edge design technique for deep, short coupling beams with a definite span-to-depth ratio of less than two, based on their test results. Nevertheless, these reinforcing details pose significant challenges during construction. Furthermore, the storey height limits the coupling beams' depth, as most coupling beams are used in at least 30-storey buildings, thereby producing a low span-to-depth ratio (usually less than 3), which the international standard codes do not explicitly state (See Fig.1.6).

FIGURE 1.6: HIGH-RISE BUILDING (30 PLUS STOREY-BUILDING) WITH SHORT COUPLING BEAMS.

The strength design of short coupling beams (SCBs) at the beam ends is limited to what is provided in Chapter 18 of the American Concrete Institute(*318-19 Building Code Requirements for Structural Concrete and Commentary*, 2019). Nevertheless, fissures begin in the middle of the beam and move outward toward its ends. Because plastic hinges were first developed at the beam's ends, they maintain their integrity even under very large displacements, preventing sliding shear failure at the beam-to-wall interface (Luciano Galano and Andrea Vignoli, 2000). Additionally, the American Society of Civil Engineers (*Seismic Evaluation and Retrofit of Existing Buildings*, 2017) only provides design codes for CRCBs, and also in (0*Eurocode 8, Design of Structures for Earthquake Resistance*, 2005), the calculation of forces and moments is done at the beam ends. The shear stress of diagonally reinforced concrete coupling beams (DRCBs) is limited to 0.83 MPa by ACI 318-19 (*318-19 Building Code Requirements for Structural Concrete and Commentary*, 2019) to prevent concrete web crushing. The shear demand of DRCBs tends to exceed this stress limit if the coupled shear walls (CSWs) designed to have a coupling ratio of ratio 0.45 to 0.6, which is generally agreed upon for CSWs to exhibit favourable seismic performance. Very few DRCBs designs will meet ACI 318-19 requirements, especially when taking into account the effects of code-prescribed torsion and redundancy factors (Fig. 1.6) (Fortney et al., 2006).

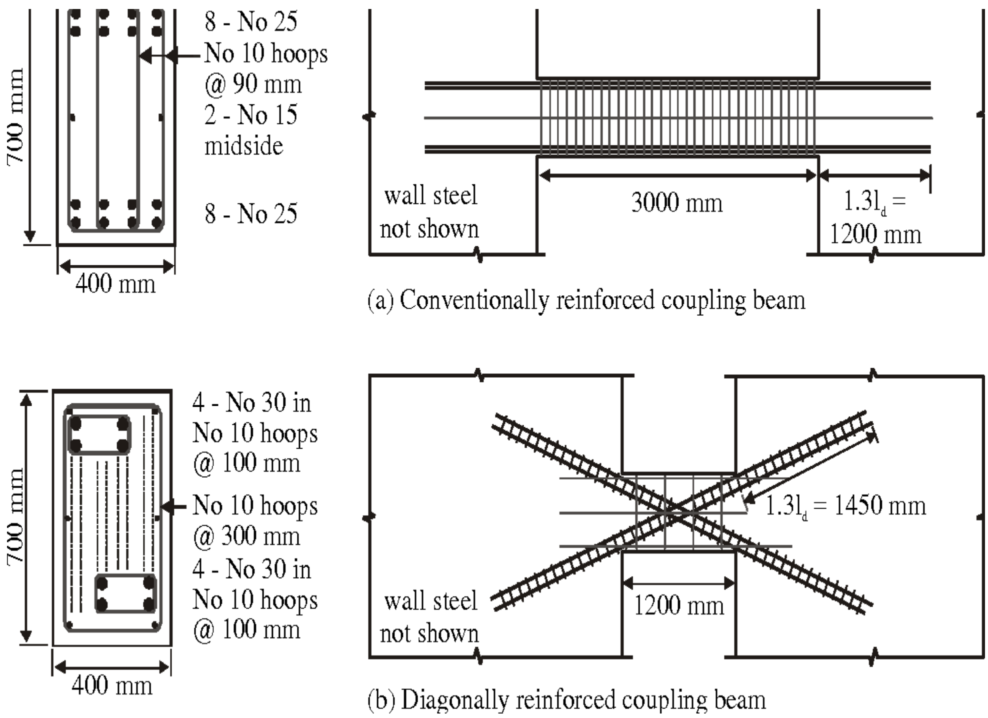

FIGURE 1.7: (A) CRCBS AND (B) DRCBS

Chapter 1: Literature Review on Coupling Beams

Short coupling beams have a low aspect ratio (Ln/h ≤ 2), they are unsuitable for design using the ordinary beam approach because of discontinuity regions (D-regions)(Monthian Setkit, 2012)(see Fig. 1.8).

FIGURE 1.8: STANDARD REINFORCEMENT DETAILING IN EARTHQUAKE-RESISTANT COUPLING BEAMS (COURTESY TO RÉMYLEQUESNE).

Investigations on reinforcement detailing alternatives, such as various rhombic configurations, have been proposed (I. A. Tegos and G. Gr. Penelis, 1988; Luciano Galano and Andrea Vignoli, 2000). However, test findings indicated that inadequate seismic behavior was found or presented substantial construction challenges when beams were linked with those reinforcing choices; the second chapter provided more details on this. Another potential alternative, consisting of steel or concrete-encased steel coupling beams (Gong & Shahrooz, 2001) showed favourable seismic behaviour. However, the need for embedding the steel section into the walls creates severe interface problems with the wall boundary reinforcement (B. A. Canbolat, G. Parra-Montesinos, J. Wight, 2005).

Along the height of the shear walls, elastic deformations happen at both ends of coupling beams as well as at the bases of walls, causing energy dissipation to occur throughout an area of a building that has coupling beams (see Figure 1.1.1).

Chapter 1: Literature Review on Coupling Beams

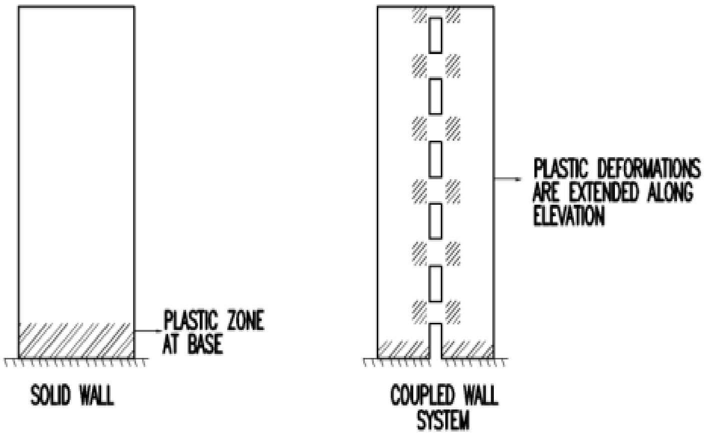

FIGURE 1.1.1: PLASTIC DEFORMATIONS ON (A) SOLID WALL AND (B) COUPLED WALL SYSTEM (COURTESY TO EMRE TOPRAK ET AL)

The earthquake loads impose the high shear stress demand (typically more than 0.5 for reinforced concrete short coupling beams). To increase the lateral force resistance of high-rise buildings (those with at least 30 stories), short coupling beams (SCBs) are usually added. They resemble deep beams in that they are thick and short, hence the term "short coupling beams" (Fantilli et al., 2009). Among the most important components of concrete buildings are SCBs. The short coupling beams (SCBs) have two major roles in most high-rise buildings; firstly, for increasing the moment of resistance, shear walls are first coupled by SCBs, which achieve this by lowering the stress on each wall face as they yield first and creating plastic hinges before the yielding of wall piers. They further disperse the tension along the element and make it easier to resist by applying lateral force along the second wall’s length (Fantilli et al., 2009)

Secondly, under severe stress, SCBs serve as a source of energy dissipation. For instance, a building needs to be able to withstand pressure in the event of an earthquake. A structure must be sufficiently flexible to be resilient; otherwise, in the event of strong earthquake, for instance, the building would collapse at the wall pier (see Fig.1.9). The coupling beam, which is intended to yield first in order to protect important structural parts in the event of excessive stress, therefore reinforces the overall design of a building.

Chapter 1: Literature Review on Coupling Beams

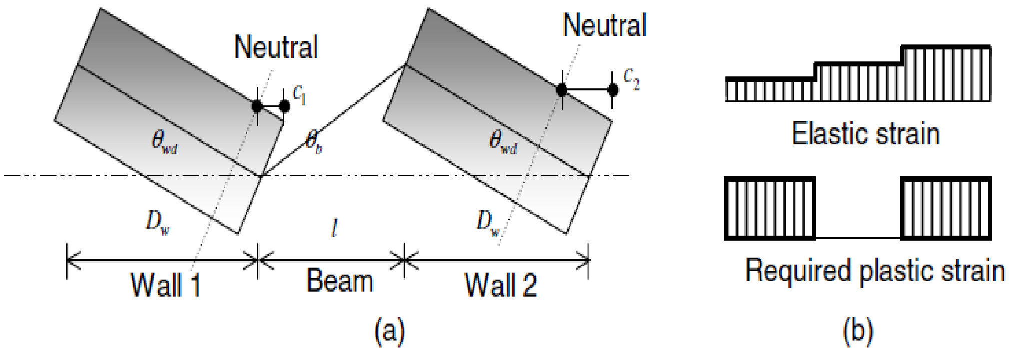

FIGURE 1.1.2 : (A) RELATIONSHIPS BETWEEN WALL AND COUPLING BEAM ROTATIONS; (B) STRAIN OF HORIZONTAL TOP CHORD OF COUPLING BEAMS (JANG & HONG, N.D.).

Where: θwd is the rotation capacity of the walls; *Dw* is the length of the wall; c1andc2are the centroid of the walls.

Presently, the design industry uses five popular kinds of coupling beams and these are CRCBs, DRCBs, steel coupling beams, encased steel composite coupling beams, and embedded steel composite coupling beams (I. A. Tegos and G. Gr. Penelis, 1988) . However, this study only includes CRCBs and DRCBs. According to Aktan and Bertero, coupling beams typically experience a high number of yield excursions and considerable inelastic end rotation demands (Aktan & Bertero, 1981). When designing short reinforced coupling beams (SCBs), the following elements must be considered to achieve a high degree of toughness and ductility (HungChung-Chan & LuWei-Ting, 2015):

1.2.1 Span-to-Depth Ratio $(\frac{Ln}{h})$

One important factor that influences beam behaviour and failure mechanisms is the aspect ratio, also known as the span-to-depth ratio, when connecting beams. Aspect ratios of less than four are typically the result of the necessary stiffness of coupling beams. As per the beam theory (Ln/h > 2), which supports the classical calculations for normal beams in the Euro code. However, since international codes do not validate SCBs (Ln/h ≤ 2), more sophisticated techniques are required (Monthian Setkit, 2012).

1.2.2 Shear Stress (V)

The span-to-depth ratio, the flexural reinforcement ratio, the flexural reinforcement's yield strength, and the strain hardening of the reinforcement, all influence the maximum shear stress (Monthian Setkit, 2012).Because the shear developed in a flexural member is directly related to the member's flexural capacity, the shear stress increases as the span length decreases (Monthian Setkit, 2012). In coupling beams, there are three classifications of shear stresses and these are:

1. Shear stress of 3√f'c psi: CRCBs, or cross-sectional reinforced concrete, function well and fail in the flexural mode (Aktan and Bertero 1981).
2. Shear stress between (3√f'c) and (6√f'c) psi: this will frequently result in a flexural-shear failure.
3. Shear stress greater than 6√f'c results in diagonal reinforcement and sliding shear as the predominant failure mode.

   Where ($\sqrt{f'c}$, psi) is the shear stress of SCBs.

1.2.3 Reinforcement Details

The arrangement of flexural and shear reinforcement plays an important role in the behaviour of coupling beams under load reversals (Monthian Setkit, 2012). Section 2.3.1 of this study delineates more information on the reinforcement arrangements of CRCBs, DRCBs and rhombic reinforcement.

1.2.4 Anchorage of Beam Flexural Reinforcement

It is crucial to anchor coupling beam reinforcement in the walls because it has an impact on how coupled wall systems behave as a whole. A substantial slip of reinforcing bars anchored in the walls could occur as a result of the large inelastic deformations anticipated at the end of the SCBs, which would be extremely detrimental to the entire reaction of CWSs (Aristizabal-Ochoa, 1983).

1.3 International Standard Codes Provisions

1.3.1 Algerian Seismic Rules RPA99/Version2003

Section7.7 Walls and Shear Walls**7.7.1** Formwork: Elements satisfying the condition l ≥ 4a are considered as sails (see Fig.1.10). Otherwise, these elements are considered linear elements('MINISTERE DE L'HABITAT (RPA99/Version20030', n.d.).

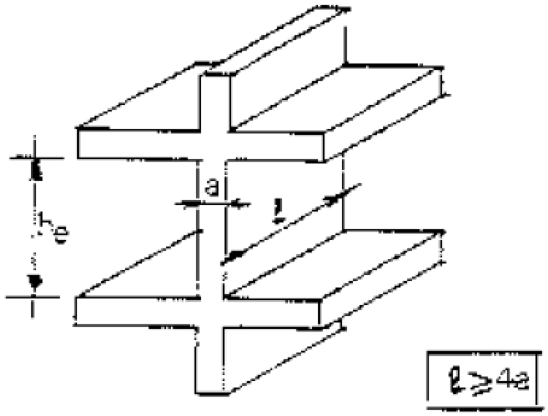

FIGURE 1.1.3: SAIL CUT IN ELEVATION (COURTESY TO RPA99V2003).

7.7.2. Shear limit stresses in lintels (coupling beams) and trumeaux (pillars)

In addition to the specifications in paragraph 7.3, the shear stress in the concrete is limited as follows:

$\tau \mathbf{b} \leq \ (\overline{\tau \mathbf{b}} = \mathbf{0.2fc28})$. (1.1)

With $\tau \mathbf{b} = \frac{V}{b0.d}$

bo: thickness of the lintel or veil

d: useful height =0.9h

h: total height of the raw section

7.7.3 Lintel reinforcements

7.7.3.1 First case: **τb≤ 0.06.fc28**

The lintels are calculated in simple bending (with the forces M, V) (‘MINISTERE DE L’HABITAT (RPA99/Version20030’, n.d.). The following parameters are considered:

- Longitudinal bending steels (Al)
- Transverse steels (At)
- Steels in the current part (skin steels) (Ac)

7.7.3.2 Second case: **τb> 0.06.fc28**

In this case, it is necessary to arrange the longitudinal reinforcements (upper and lower), transverse and in common areas (skin reinforcements) following the regulatory minimums(‘MINISTERE DE L’HABITAT (RPA99/Version20030’, n.d.). The forces (M,V) are taken up along the diagonal rods (compression and traction) along the average axis of the diagonal reinforcements AD to be arranged obligatorily (see Fig.1.1.4 and Fig.1.1.5).

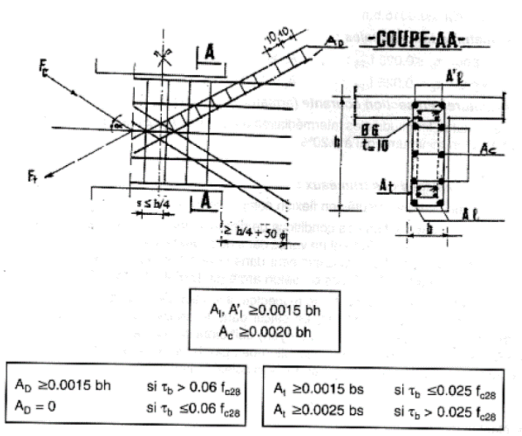

FIGURE 1.1.4: LINTEL (COUPLING BEAM) REINFORCEMENT (RPA99/V2003)

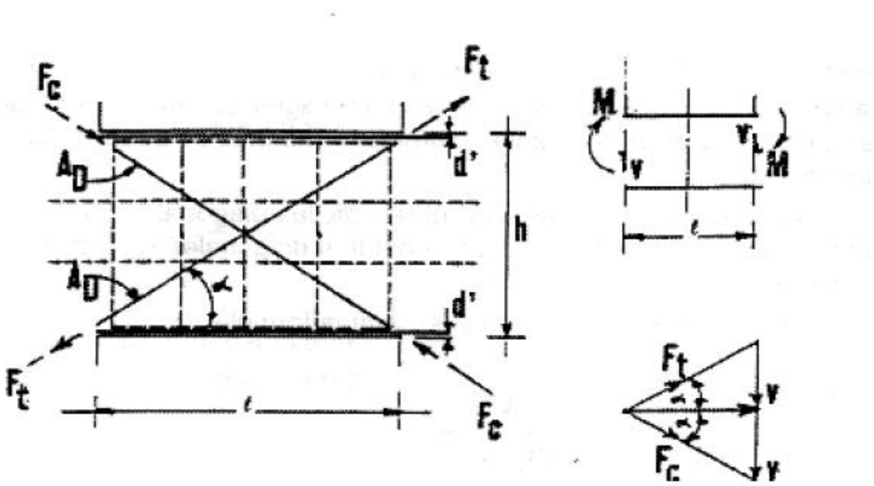

FIGURE 1.1.5: FORCES IN THE LINTEL CONNECTING RODS (RPA99/V2003).

1.3.2 Euro Code 8 (EC8)

EC8 5.5.3.5 Coupling elements of coupled walls

According to section 5.5.3.1 which applies only to coupling beams that meet one of the following conditions (*Eurocode 8, Design of Structures for Earthquake Resistance*, 2005):

a) Cracking along both diagonals is improbable. A rule of appropriate application is valid for CRCB:

$VEd \leq fctd.bw$ (1.2)

Where: VEd is the design shear force for the seismic design condition that results from the study (or it is the coupling element's design shear force). *f*ctd is the design value of the tensile strength of concrete, in accordance with EN 1992-1-1:2004 and bw is the width of the web of a beam and d is the effective depth of section (*Eurocode 8, Design of Structures for Earthquake Resistance*, 2005) .

b) There is assurance of a dominant flexural mechanism of failure. The following application rule is acceptable: l/h > 3.

According to section 5.5.3.5 (3**)** of the EC8**,** reinforcement placed along both diagonals of the beam, in accordance with the following, ought to be applied to offer resistance to seismic activity if neither of the requirements in **5.5.3.5.(2)** is satisfied:

a) It is important to ensure that the following equation is satisfied for DRCB:

$$VEd \leq 2.Asi.\,fyd.\sin\alpha \quad (1.3)$$

Where VEd is the coupling element's design shear force and Asi denotes the total area of steel bars in each diagonal direction. The angle α is between the beam's axis and the diagonal bars (see Fig.1.14).

b) The diagonal reinforcement is placed in column-like components with side lengths at least equivalent to 0.5bw. The anchoring length should be 50% higher than EN 1992-1-1:2004 [EN 1992-1-1 (2004) (English): Euro code 2: Design of Concrete Structures, Part 1-1: General Building Rules].

c) Provide hoops around column-like parts to prevent longitudinal bars from buckling. The provisions of 5.5.3.2.2(12) apply to the hoops.

d) Provide longitudinal and transverse reinforcement on both lateral faces of the beam to fulfil EN 1992-1-1:2004 minimum criteria for deep beams. Only 150 mm of longitudinal reinforcement should be used, and it should not be fixed in adjacent walls.

Chapter 1: Literature Review on Coupling Beams

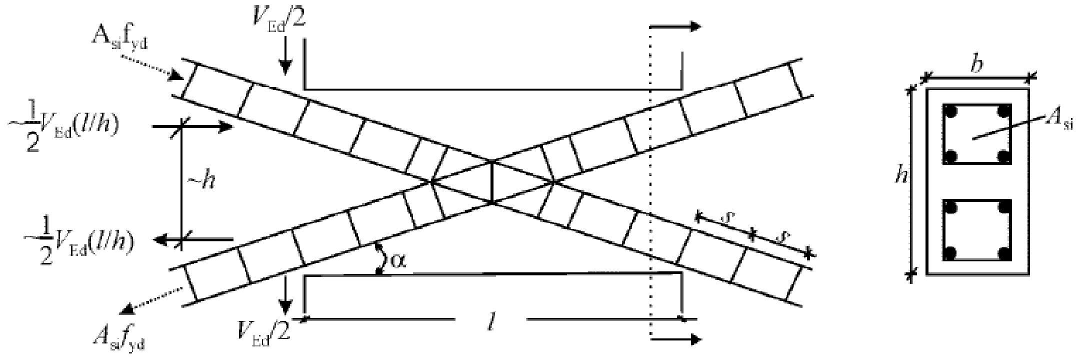

FIGURE 1.1.6: DIAGONALLY REINFORCED COUPLING BEAM (EURO CODE 8)

1.3.2 ACI 318-14 Building Code

Section 18.10.7.1 states that coupling beams with aspect ratio (ℓn/h ≥ 4) must meet 18.6.2.1's requirements, with the wall boundary being regarded as a column. It is not necessary to comply with the requirements of 18.6.2.1(b) and (c) if an analysis demonstrates that the beam has sufficient lateral stability.

Coupling beams in Section 18.10.7.2 with (ℓn/h) < 2 and with the following equation:

$Vu \geq 4.\lambda.f\ c.Acw$ (1.4)

Where Vu is the shear demand in coupling beams, symmetrically around the mid-span, two intersecting groups of diagonally arranged bars, ought to be applied to reinforce.

To design coupling beams with span-to-depth ratios greater than to 2.0 and less than 4.0 (2.0 $< ln/h <$ 4.0) ACI 318-14 provides two options (*Building Code Requirements for Structural Concrete (ACI 318-14) [and] Commentary on Building Code Requirements for Structural Concrete (ACI 318R-14)*, 2014).

According to Section 18.10.7.2 coupling beams in the 2.0 ≤ ln/h < 4.0 range can be designed as coupling beams with diagonal reinforcement or as beams of special moment resisting frames as per Section 18.6 of ACI 318-14. Section 18.6.2.1 states that beams must fulfil (a) through (c):

(a) The minimum clear span ℓn is 4d. (b) The minimum width bw is the lesser of 0.3h and 10 inch. (c) The beam width projection on each side that is wider than the supporting column's width cannot be greater than the smaller of c2 and 0.75c1.

Section 18.10.7.3 states that coupling beams that are not subject to 18.10.7.1 or 18.10.7.2 may be strengthened in accordance with 18.6.3 through 18.6.5, where the wall border is considered a column, or with two intersecting groups of diagonally positioned bars symmetrical around the mid-span.(*Building Code Requirements for Structural Concrete (ACI 318-14) [and] Commentary on Building Code Requirements for Structural Concrete (ACI 318R-14)*, 2014). Furthermore, coupling beams reinforced with two intersecting groups of diagonally positioned bars symmetrical about the mid-span shall meet the requirements stated in Section 18.10.7.4:

(a) Vn will be determined using:

$$Vn = 2.Avd.fy.\sin\alpha \leq 10.f'c.Acw \quad (1.5)$$

Where Vn is the calculated nominal shear strength and α is the angle formed by the coupling beam's longitudinal axis and diagonal bars.

(b) There must be a minimum of four bars in each group of diagonal bars, provided in two or more layers. For the yield strength (fy) in tension, the diagonal bars must be inserted into the wall at least 1.25 times the development length.

(c) Rectilinear transverse reinforcement with out-to-out dimensions of at least $\frac{bw}{2}$ in the direction parallel to bw and $\frac{bw}{5}$along the other sides, where bw is the web width of the coupling beam, must encircle each group of diagonal bars. Under seismic loading, deep coupling beams may be subject to shear control and deterioration of strength and stiffness (Paulay, 2011).

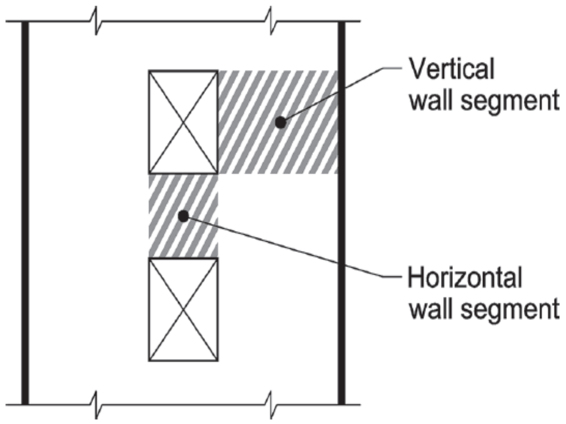

FIGURE 1.1.7: WALL WITH AN OPENING (ACI 318-14).

Research demonstrates that diagonally oriented reinforcement works best when the bars are positioned at a significant inclination. Therefore, beams with aspect ratios of ∓ Ln/h < 4 are the only ones that can have diagonally reinforced coupling beams. The diagonal bars in the beam cross-section should be arranged in two or more layers, roughly symmetrically. The diagonally positioned bars are meant to supply the beam's whole shear and matching moment strength. These provisions do not apply to designs that derive their moment strength from combinations of longitudinal and diagonal bars(*Building Code Requirements for Structural Concrete (ACI 318-14) [and] Commentary on Building Code Requirements for Structural Concrete (ACI 318R-14)*, 2014).

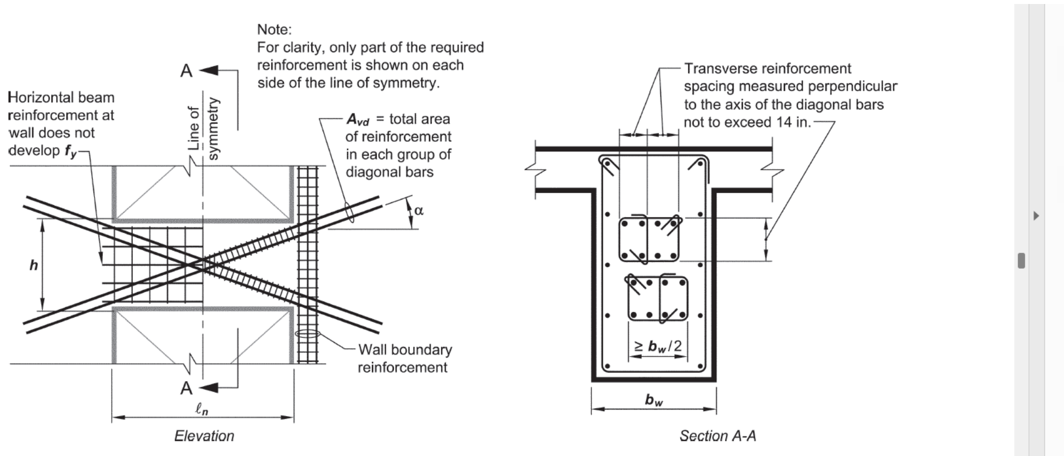

FIGURE 1.1.8: CONFINEMENT OF INDIVIDUAL DIAGONALS OF DRCB (ACI 318-14).

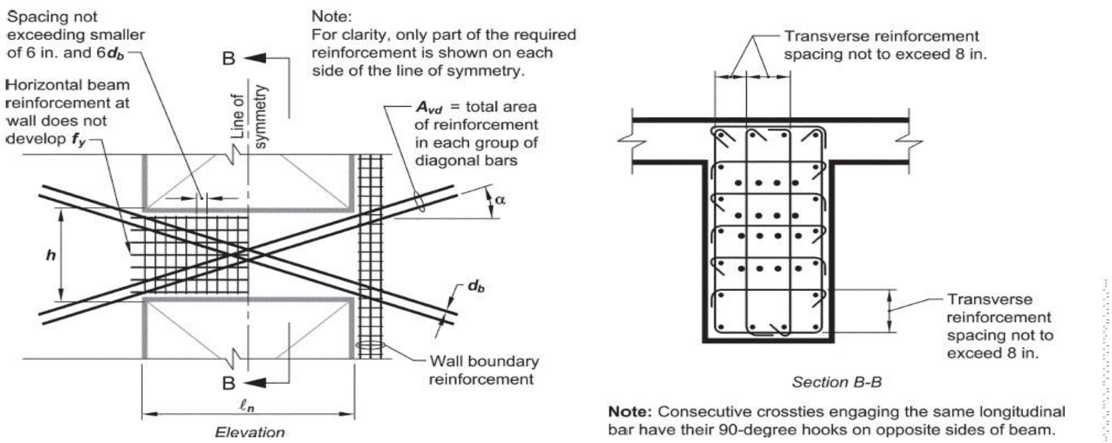

FIGURE 1.1.9: FULL CONFINEMENT OF DIAGONALLY REINFORCED CONCRETE BEAM SECTION (ACI 318-14).

1.3.3 ACI 318-19

Structural wall coupling beams can dissipate energy and offer stiffness (see Fig.1.11)(*318-19 Building Code Requirements for Structural Concrete and Commentary*, 2019).

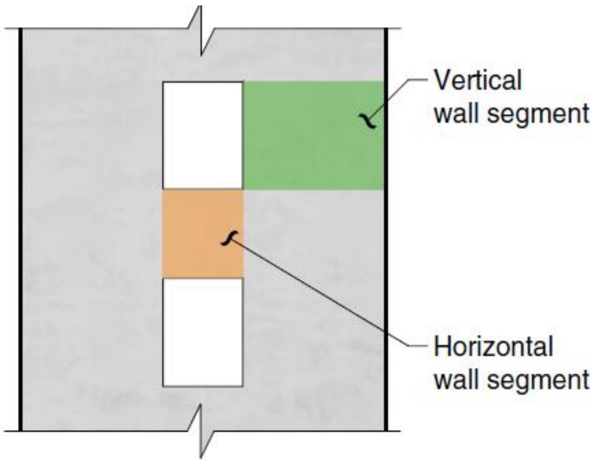

FIGURE 1.1.10: WALL WITH AN OPENING (ACI 318-19).

Section 18.10.7.1 states that coupling beams with an aspect ratio (Ln/h) of at least four must meet the 18.6 requirements, with the wall boundary being regarded as a column 18.10.7.2), the aspect ratio (Ln/h) which is less than two and with:

$$Vu \geq 4.\lambda\sqrt{f'c}.Acw \quad (1.6)$$

Where Vu is the shear strength of the coupling beams, the number 4 signifies the minimum number of diagonal bars allowed in each diagonal group. Additionally, Acw is the cross-sectional area of the beam, λ is the security coefficient and f`c represents the specified compressive strength of concrete.

According to equation (1.7) , coupled beams are reinforced with two intersecting groups of diagonally arranged bars symmetrical about the mid-span unless it can be demonstrated that the structure's ability to support loads will not be hampered by the coupling beams' loss of stiffness and strength. Connecting beams with two intersecting sets of bars are positioned diagonally around the mid-span. To meet the following conditions, the mid-span must:
(a)The following formula will be used to determine Vn:

$$Vn \ = \ 2.Avd.fy.sin\alpha \leq \ 10.\sqrt{\ } \left(f \ \grave{}c\right).Acw \quad (1.7)$$

Where Vn is the calculated nominal shear,α represents the angle made up of the diagonal bars, longitudinal axis of the coupling beam and Avd denotes the total area of reinforcement in each diagonal bars.

(b) Each group of diagonal bars, provided in two or more layers, must contain a minimum of four bars.
(c) Each group of diagonal bars must be encircled by rectilinear transverse reinforcement with out-to-out dimensions of at least $\frac{bw}{2}$in the direction parallel to bw and $\frac{bw}{5}$ along the other sides. Where bw is the coupling beam’s web width, (see Fig.1.12).

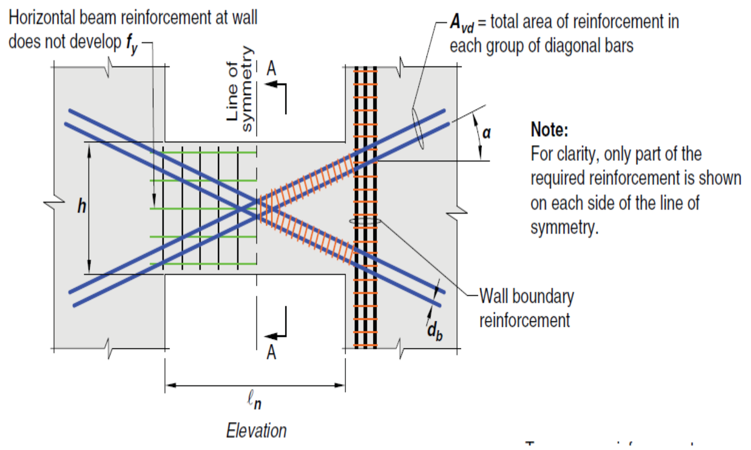

FIGURE 1.1.11: DIAGONAL REINFORCED COUPLING BEAM (ACI 318-19).

18.10.9.3 In the direction under consideration, coupling beams must meet 18.10.7 and (a) through (c) requirements:

a) Coupling beams at all building levels must have Ln/(h) ≥2;
b) In at least 90% of the building's levels, every coupling beam at a floor level must have $\frac{Ln}{5} \leq 5$.
c) Every coupling beam must meet the specifications of 18.10.2.5 at both ends.

FIGURE 1.1.12: RCC COUPLING BEAM DESIGN AS PER ACI

1.3.4 ASCE-41-17 (American Society of Civil Engineers)

A beam element that accounts for both shear and bending deformations must be employed to simulate coupling beams. The loss of shear strength and stiffness during reversed cyclic loading to large deformations must be accounted for by the element's inelastic response (*Seismic Evaluation and Retrofit of Existing Buildings*, 2017). Coupled beams with diagonal reinforcement meeting ACI 318 specifications may only use a beam element that represents flexure. The effective stiffness values for coupling beams in Fig.1.20 are for non-pre-stressed beams unless a more thorough analysis identifies a different stiffness.

Component	Flexural Rigidity	Shear Rigidity	Axial Rigidity
Beams-non Prestressed	0.3EcEIg	0.4EcEAw	-
Beams-Prestressed	EcEIg	0.4EcEAw	-
Columns-with compression caused by design gravity	0.7EcEIg	0.4EcEAw	EcEAg
Beam-Column Joints	-	0.4EcEAg	EcEAg

Figure 1.1.13: Effective stiffness value of coupling beams (ASCE-41-7).

The following method shall be allowed for structural walls and wall segments that exhibit inelastic behaviour under lateral loading controlled by flexure (see Fig.1.21). The load-deformation relationship shown in Figure 1.1.14 will be applied, and the rotation over the plastic hinging region at the member's end will be measured along the x-axis of the figure.

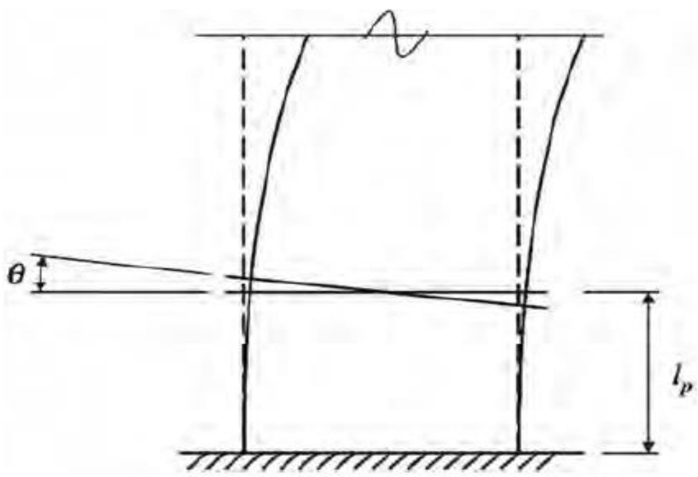

Figure 1.1.14: Plastic hinge rotation in the shear wall, where flexure dominates inelastic response (ASCE-41-17).

Equation (10) is applied to determine the yield point, θy, as shown in Fig. 1.1.14.

$$\theta y.E \; = (\frac{MyE}{(EI)eff}).lp \quad (1.8)$$

Where lp = Assumed plastic hinge length.

The following method shall be allowed for coupling beams (see Figure 1.1.15).

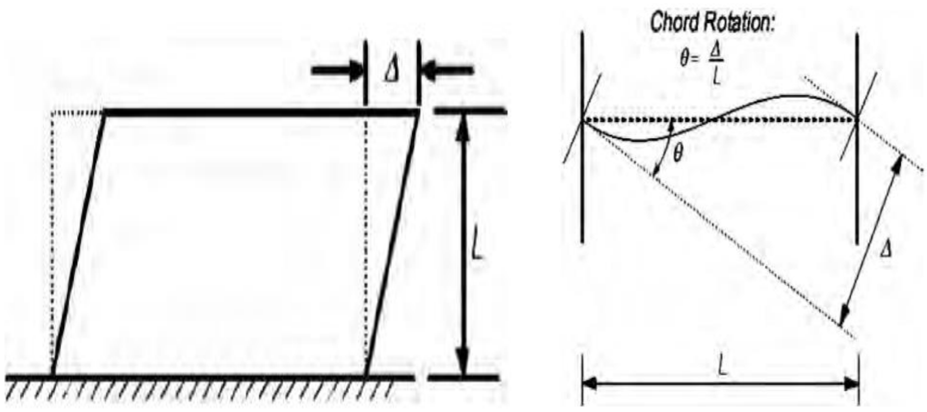

(a) **(B)**

*FIGURE 1.1.15 :(**A**) STORY DRIFT IN A STRUCTURAL WALL WITH INELASTIC RESPONSE PREDOMINATING SHEAR*

(B) *CHORD ROTATION FOR STRUCTURAL WALL COUPLING BEAMS (ASCE-41-17).*

The formula for nominal joint shear strength VJ will be determined by applying ACI 318's general procedures, modified by Equation *1.9 and 1.10*

$$Vj = \lambda y.\sqrt{\frac{f'c}{E}}.Aj(\frac{lb}{in^{\wedge}2}) \quad (1.9)$$

$$Vj = 0.083.\lambda y..\sqrt{\frac{f'c}{E}}.Aj(MPa) \quad (1.10)$$

1.3.5 IS13920 (2016) - (Indian Standard Institution)

For diagonal reinforcement detailing, IS 13920 (2016) is utilized following clause 10.5-page no. 16. The shear stress τve caused by an earthquake should not surpass the following equation:

$$\tau ve > 0.1 * \sqrt{fck} * (\frac{Ls}{D}) \quad (1.11)$$

Where Ls is the clear span of the coupling beam and D is the overall depth.

The following formula can be used to calculate the area of this diagonal reinforcement:

$$Ast = \frac{Vu}{1.74} * fy * \sin\alpha \quad (1.12)$$

Where: fy is the yield strength, Vu is factored shear force, and Ast is an area of diagonal reinforcement.

An inclination of the diagonal reinforcement in the coupling beam is the stress of the steel reinforcing bar. There should be a minimum of four bars with an 8 mm diameter along each diagonal. Every diagonal's longitudinal bars must be surrounded by transverse reinforcement spaced no more than 100 mm apart. The coupling beam's diagonal bar must be tensioned and anchored 1.5 times the development length in the adjacent wall. Where bw is the beam's width and D is the beam's depth (Takale & Taware, 2023).

1.4 Advanced Methods

1.4.1. The Strut and Tie Method (STM)

Researchers and practitioners now believe that the truss model is a reasonable and suitable foundation for designing cracked reinforced concrete beams loaded with bending, shear, and torsion (Schlaich et al., 1987). When designing structural concrete members or member areas where geometric discontinuities or load induces a nonlinear distribution of longitudinal stresses inside the cross section, the STM is utilised. The idealized truss has nodes for the joints, ties for the tension members, and struts for the compression members. A concentrated load or reaction, or a change in a structural element's geometry, can cause a discontinuity in the stress distribution.

According to St. Venant's principle, the stresses brought on by bending and axial force approach a linear distribution at a distance from the discontinuity that is roughly equal to the member's total depth, h. Hence, discontinuity regions are presumed to extend h from the section containing the load or geometry change(*318-19 Building Code Requirements for Structural Concrete and Commentary*, 2019). The strut-and-tie design method is used in this case, assuming that D-regions can be analysed and designed using hypothetical pin-jointed trusses composed of struts and ties connected at nodes (Fig. 1.23).

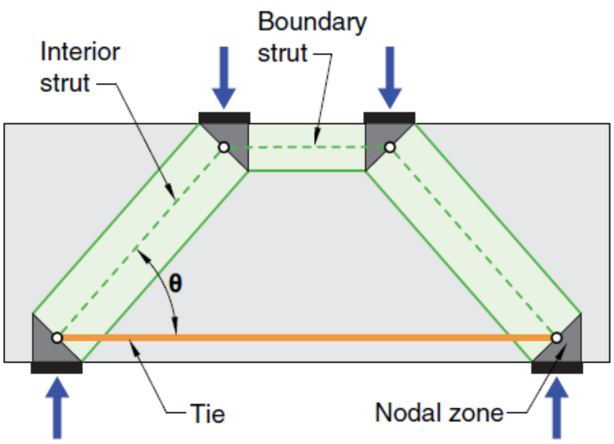

FIGURE 1.1.16: DESCRIPTION OF STRUT AND TIE METHOD (ACI 318-19)

The following four steps make up the strut-and-tie method, which is the process of creating a strut-and-tie model to support the imposed forces acting on and within a D-region:

(1) Characterize and separate every D-region.
(2) Determine the forces that arise on each D-region boundary.
(3) To transfer the resulting forces throughout the D-region, choose the model and calculate the forces in the struts and ties.
(4) Make sure the nodal zones, ties and struts are designed with enough strength. The effective concrete strengths are taken into consideration when determining the strut and nodal zone widths.

Truss action resists shear forces that are primarily applied to the coupling beam through loading(Jang & Hong, n.d.).The components of strut-and-tie models are ties and struts joined at nodes to create an idealized truss in two or three dimensions (see Figure 1.17).

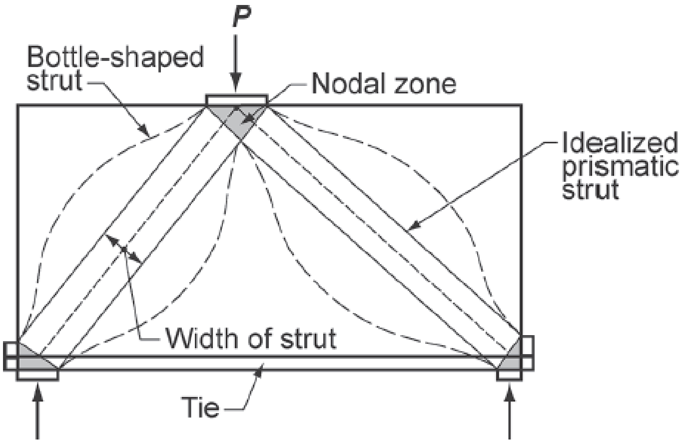

FIGURE 1.1.17: DESCRIPTION OF STRUT-AND-TIE MODEL (ACI 318-14).

The following equation must be satisfied by brackets and corbels with shear span-to-depth ratios ($\frac{av}{d}$< 2.0) that are designed using the strut-and-tie method. Where av represents the clear span and d is the depth of the beam.

$$Asc \geq 0.04(\frac{f'c}{fy}).bw.d \qquad (1.13)$$

Where: Asc is the area of primary tension reinforcement in a corbel or bracketin^2, bw is the web width or diameter of circular section and d is the distance from extreme compression fibre to centroid of longitudinal tension reinforcement.

The design strength of every strut, tie, and nodal zone in a strut-and-tie model must meet equation (1.14) for every applicable factored load combination:

$$\varphi n.Sn \geq U \qquad (1.15)$$

Where φn denotes the strength reduction factor, Sn represents the nominal moment, shear, axial, torsion or bearing strength and U is the strength of a member or cross section required to resist factored loads or related internal moments.

Chapter 1: Literature Review on Coupling Beams

The design of every strut, tie and nodal zone includes the following (a) through (c):

(a)Nodal zones : φn.Sn≥Fus

(b)Ties : φn.Fnt≥Fut

(c) Struts: φ.Fnn≥ Fus

Where Fus is the factored compressive force in a strut, Fut is the factored tensile force in a tie, Fnt is the nominal strength of a tie and Fnn represents the nominal strength at face of a nodal zone.

The effective compressive strength of concrete in a strut, fce is calculated by:

$$fce = 0.85.\beta c.\beta s \qquad (1.16)$$

Where, the number 0.85 represents the coefficient of security,s is the factor used to account for the effect of cracking and confining reinforcement on the effective compressive strength of the concrete in a strut. **β**c is the confinement modification factor for struts and nodes in a strut-tie-model (318-19 Building Code Requirements for Structural Concrete and Commentary, 2019).

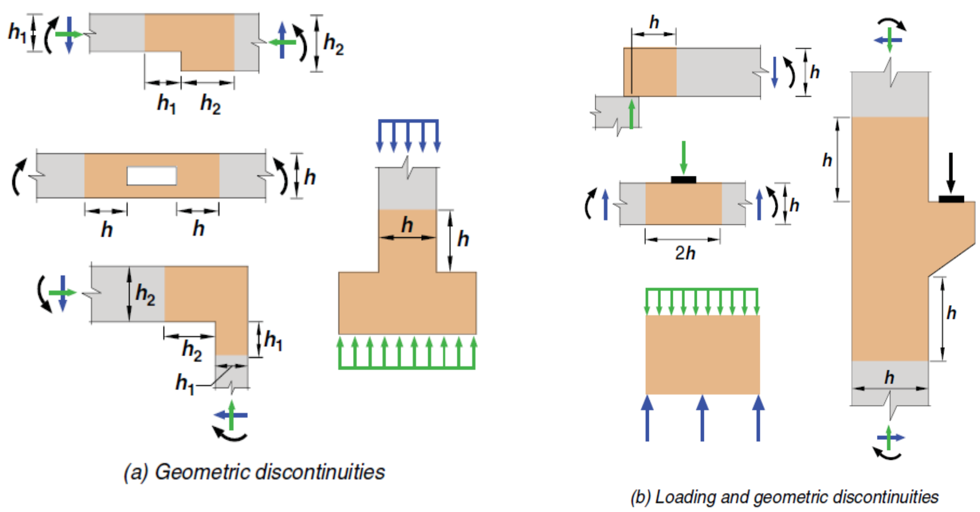

FIGURE 1.1.18: (A) AND (B) D-REGIONS AND DISCONTINUITIES (COURTESY TO ACI 318-19).

All factored loads must be able to be transferred by strut-and-tie models to nearby B-regions or supports. In strut-and-tie models, the internal forces balances the applied loads and reactions.

It is acceptable for struts and other ties to cross. Additionally, struts can only cross over or intersect at nodes (see Fig.1.26).

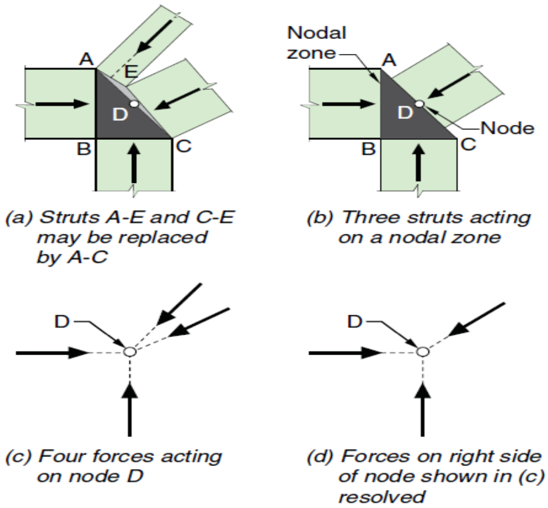

FIGURE 1.1.19: RESOLUTION OF FORCES ON A NODAL ZONE (COURTESY TO ACI 318-19).

The design strength of every strut, tie, and nodal zone in a strut and tie model must meet φ (the strength reduction factor) for every applicable factored load combination Fnn ≥Fus. The dimension at the ends of the strut that is perpendicular to its axis is known as the width of the strut, or ws, and is used to compute Acs (*318-19 Building Code Requirements for Structural Concrete and Commentary*, 2019). A strut's nominal compressive strength, Fns, can be computed using either (a) or (b):

(a) A strut lacking longitudinal support:

$$Fns = fce.Acs \qquad (1.17)$$

Where: Fns is the strut's nominal compressive strength, fce is effective compressive strength of concrete in a strutand Acs is the cross-sectional area at one end of a strut in a strut-tie-model, taken perpendicular to the axis of the strut.

(b) Strength of Strut with longitudinal reinforcement:

$$Fns = fce.Acs + As.f'c \qquad (1.18)$$

Fns is evaluated at each end of the strut and it is taken as the lesser value and f'c is the specified compressive strength of concrete.

Equation (1.19) is intended to preclude diagonal tension failure. In discontinuity regions, diagonal tension strength increases as the strut angle increases. For very steeply inclined struts, Vu can exceed $10.\lambda\lambda s\sqrt{f'c}$ .bw.d:

$$Vu \leq \varphi 5\ tan\varphi\lambda\lambda s\ .f'c.bw.d \qquad (1.20)$$

Where Vu is the maximum factored two-way shear stress calculated around the perimeter, λ denotes the modification factor, λs is the factor used to modify shear strength and d is the distance from extreme compression fibre to centroid of longitudinal reinforcement.

1.4.1.2 Equilibrium Condition

One may envision effective structural systems when apertures (openings) are arranged in a regular and logical mode. These systems are especially well-suited for ductile response with very good energy dissipation characteristics, these are coupling beams in particular (Jang & Hong, n.d.). These coupling beams can then be subjected to enough rotations by the walls, which act primarily as cantilevers, to create yield. The beams can disperse energy throughout the entire height of the structures if they are appropriately detailed. It can be observed that, in the conventional form, flexural stresses resist the total overturning moment, M0, at the base of the cantilever, while axial forces and moments resist it in the coupled walls (Jang & Hong, n.d.). These satisfy the following basic equilibrium statement:

$$M = M1 + M2 + lT \qquad (1.21)$$

Where M is the total moment at the base, M1, M2 are moments at each wall pier and l is the distance between the coupled walls. The letter T denotes the force at the base of the building.

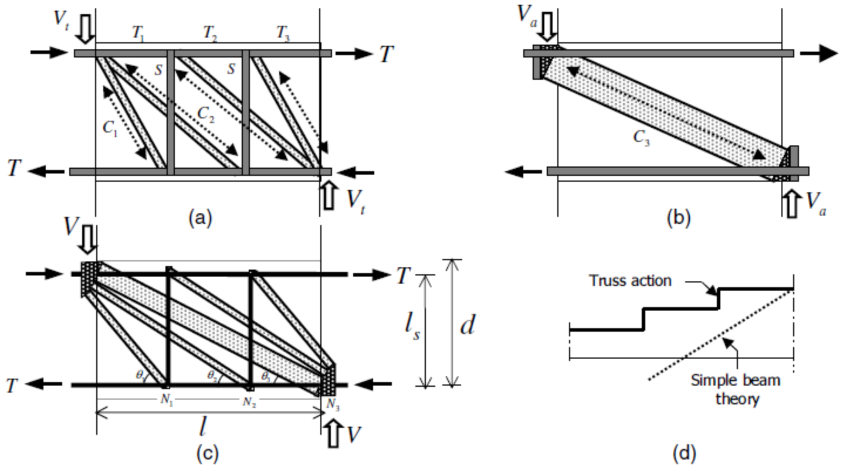

FIGURE 1.1.20: (A) TRUSS ACTION, (B) ARCH ACTION, (C) STRUT-AND-TIE MODEL, AND (D) TENSILE FORCE OF THE TOP STEEL.

The truss mechanism's diagonal strut C1 can be obtained by applying the equilibrium condition at Node N1.

$$C1 = \frac{S}{\sin\theta 1} = \frac{Av.fyv}{\sin\theta 1} \qquad (1.22)$$

Where Av and fyv are the area and yield strength of the vertical reinforcements in the coupling beam, respectively; S is the stirrup force; and θ1 is the diagonal strut's inclination angle.

The following equation (1.23) calculates the middle section of the bottom chord's horizontal tie force:

$$T1 = T1 - S.cot\theta 1 = As.fyh - S.cot\theta 1 \qquad (1.24)$$

Where fyh is the horizontal reinforcement's yield strength and T1 is the tie force of the bottom chord's left section. Likewise, at node N2, the right tie force T3 and the diagonal strut force C2 are:

$$C2 = \frac{S}{\sin\theta} \qquad (1.25)$$

$$T3 = T2 - S.cot\theta 2 \quad (1.26)$$

Where θ2 is the inclination angle of the diagonal strut.

Shear rotations by the truss action, as shown in Fig 1.1.21 (a):

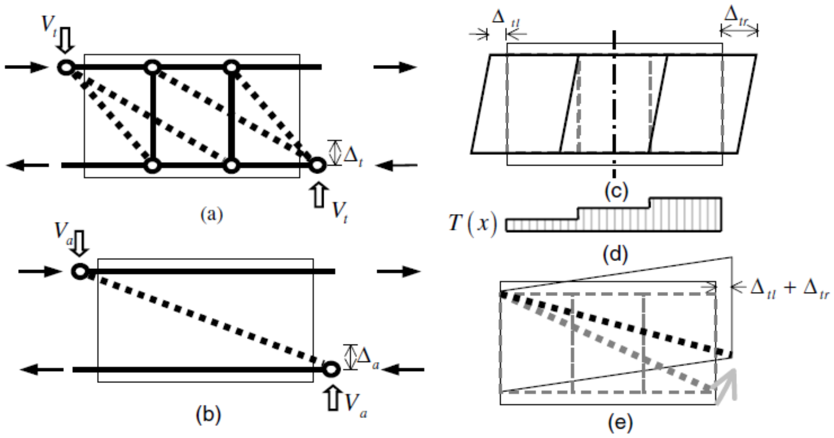

FIGURE 1.1.21: (A) DISPLACEMENT BY TRUSS ACTION; (B) DISPLACEMENT BY ARCH ACTION; (C) DISPLACEMENT BY FLEXURAL ROTATION; (D) TOP CHORD STRAIN AND (E) DISPLACEMENT BY BEAM ELONGATION.

The estimated flexural rotation is:

$$\theta fr = \frac{\Delta tl - \Delta tr}{Ls} \qquad (1.27)$$

Where: Δtl is the horizontal displacement of the left portion of the flexural reinforcement, and Δtr is the horizontal displacement of the right portion.

The shear strength of the coupling beam at the ultimate deformation is given by the following equation:

$$Vu = C1.sin\theta 1 + C2.sin\theta 2 + C3u.sin\theta 3 \qquad (1.28)$$

Where C3 is the diagonal strut force: C3u = f2. *bb*.wc3

1.4.2 The Compatibility Stress Field Method (CSFM)

The Compatible Stress Field Approach (CSFM) is a 2-D continuous finite element (FE)-based stress field analysis method that incorporates kinematic considerations in addition to traditional stress field solutions, meaning that the structure's state of strain is assessed throughout (Mata Falcón et al., 2022). This method (CSFM) enables the automatic design and evaluation of structural concrete members such as beams, walls, and in particular, discontinuity regions (D-regions) subjected to plane loading (see Figure.1.28). In addition, to other advantages, this approach allows for the accurate consideration of the load-deformation behaviour of the components by accounting for tension stiffening. This makes it possible to: (i) automatically calculate concrete's effective compressive strength (f'c) based on the transverse strain condition, much like in compression field studies that take compression softening into consideration; (ii) take into consideration the stiffening tension in-order to accurately- depict the load-deformation behaviour of the constituents. Moreover, kinematic factors, as well as more abstruse material component interactions are added to classical stress fields in the CSFM. Among other advantages, this makes it possible to closely mimic the load-deformation behaviour of the elements by accounting for tension stiffening (Mata Falcón et al., 2022). The CSFM takes into account the equilibrium at the cracks as well as the average strains of the reinforcement and assumes that imaginary, rotating, stress-free cracks open without slip (see Figure 1.1.22).

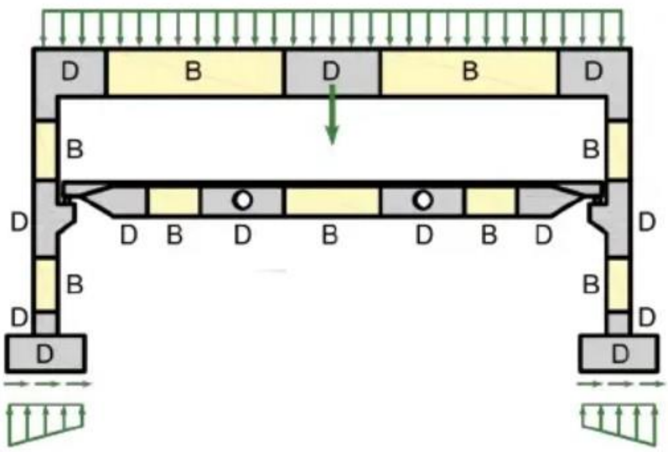

FIGURE1.1.22 :DISCONTINUITY REGIONS (NAVRATIL ET AL., 2017)

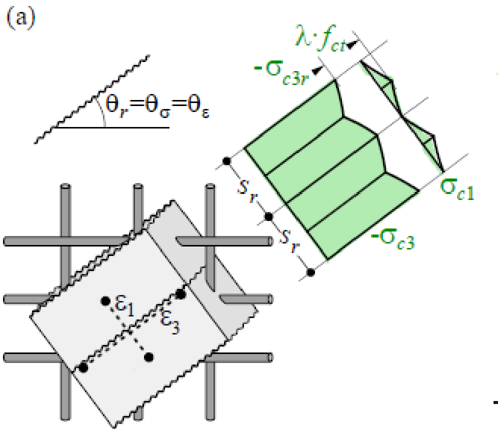

FIGURE 1.1.23 : PRINCIPAL STRESSES IN CONCRETE AND REINFORCEMENT (MATA FALCÓN ET AL., 2022).

The model of tension stiffening makes a distinction between stabilized crack patterns and those that are not. The design codes' bilinear stress-strain diagram idealizes the bare (unbounded) reinforcement. Equation (1.29) gives the value of this minimum reinforcement:

$$pcr = \frac{fct}{fy-(n-1).fct} \qquad (1.30)$$

Where *fy*= reinforcement yield strength; fct= concrete tensile strength; and $n = \frac{Es}{Ec}$= modular ratio. In the case of conventional concrete and reinforcing steel, ρcr is approximately 0.6%. Note: that ρcr is roughly seven times the minimum shear reinforcement required by the current design concrete codes:

$$pw,\min = \frac{0.08\sqrt{f'c}}{fyw} \qquad (1.31)$$

Where fyw= stirrups yield strength and *f*c= concrete compressive strength.

Conversely, the key processes for elements like aggregate interlock, residual tensile stresses at the crack tip, and dowel action—all of which depend directly or indirectly on the tensile strength of the concrete—are ignored, the CSFM is not appropriate for thin elements without transverse reinforcement (Kaufmann et al.,2020, 2020)

1.5 Conclusion

The beam theory is not valid to provide sufficient shear strength in discontinuity regions, which can include frame joints, areas with point loads, areas with abrupt changes in cross-section geometry, and areas with openings (coupling beams). The diagonally reinforced coupling beams are extremely difficult to construct, primarily because of the complicated reinforcement detailing and excessive number of diagonal bars required by the code. The strut-and-tie method (STM), which is the most popular advanced technique, can be extremely conservative in comparison to other techniques. The CSFM is more liberal and fast-paced and the application of CSFM in engineering practice is appropriate since it applies basic uniaxial constitutive rules found in concrete standards.

Chapter 2: Previous Experimental Studies On Coupling Beams

Chapter 2: Previous Experimental Studies On Coupling Beams

2.1 Introduction

This chapter gives an amplified review of experimental studies carried out on coupling beams by different scientists in previous years. Section 2.1 included a brief assessment of the rationale behind the experiments carried out by different scientists. Details on various testing variables are presented in Section 2.2. Moreover, section 2.3, extended information on the experimental evidence, taking into consideration various reinforcement configurations. After that, the reinforcement arrangement and experimental data from several scientists were discussed in relation to each testing variable.

2.2 Motives behind the Experimental Studies

Two of the biggest issues facing both developed and developing nations are the increase in population density and the scarcity of land in urban areas. The structural designers turned to high-rise structures, which are becoming more and more common, with a variety of architectural layouts, to help alleviate these issues. For all land-based structures situated in seismically active areas, earthquakes pose the greatest threat to their structural integrity. Coupling beams were typically designed with conventional (traditional) reinforcement, which included dispersed horizontal bars, vertical stirrups, and longitudinal flexural bars, before the 1964 Alaska earthquake. Due to insufficient shear capacity, it was discovered that CRCBs had suffered significant damage following the 1964 Alaskan earthquake. Subsequently, a great deal of research was carried out, to figure out how CRCBs behave seismically.

The worry regarding CRCBs' insufficient ductility resulted in the study of other reinforcement arrangements. Furthermore, there are no explicit guidelines provided by the international standard codes governing the earthquake-resistant design of coupled shear walls. For instance, only coupled shear walls are recognized by the ACI 318-14, Euro code 8, ASCI41, RPA99/v2003 and ACI 318-19 as an option. Very few design guidelines for coupling beams, particularly diagonally reinforced concrete coupling beams, have been employed. Even with the allowance of alternative full beam section confinement under ACI 318-14 section 18.10.7 4(d) to mitigate congestion issues in DRCBs, the diagonal bars remain difficult to pass through the hoops and crossties. Santhakumar's research revealed that the ACI equations were not producing the expected realistic stiffness assessment. Since practical application necessitates further research and elaboration, coupling beams have been the subject of intensive study since the 1970s (Santhakumar, n.d.).

2.3 Testing Variables Used to Analyse Coupling Beams in Previous Experimental Studies

The main objective of the experimental studies carried out by different scientists was to evaluate the seismic behaviour of coupling beams with different parameters. The following testing variables were considered to assess the performance of coupling beams:

i. The ratio of the span length divided by the depth is known as the span-to-depth ratio or the aspect ratio (Ln/h). It is a crucial parameter because, as was previously mentioned in Section 1, it can have an impact on structural behaviour, construction costs, and aesthetics.

ii. Reinforcement configuration: The arrangement of the coupling beam's primary reinforcement was one of the key testing variables used to evaluate the coupling beams' performance. Conventional and diagonal reinforcements are the primary reinforcement configurations taken into consideration. Nevertheless, as the ensuing sections make clear, there were additional reinforcement options put forth in the experimental investigations.

iii. Spacing of transverse reinforcement ratio of transverse to longitudinal reinforcement.

Most of the above-mentioned variables were incorporated in the assessment of reinforcement configuration therefore; there was no individual evaluation of the testing of some variables

Chapter 2: Previous Experimental Studies On Coupling Beams

2.3.1 Reinforcement Configuration

2.3.2 Conventionally Reinforced Coupling Beams (CRCBs)

Santhakumar defines conventionally reinforced beams (CRCBs) as spandrel beams. These have stirrups (transverse reinforcement) for shear and horizontal bars for flexure (Fig. 2.1). This type of reinforcement configuration has been the subject of numerous studies, which have demonstrated that it is susceptible to shear and diagonal failure under cyclic loads (Santhakumar, n.d.).

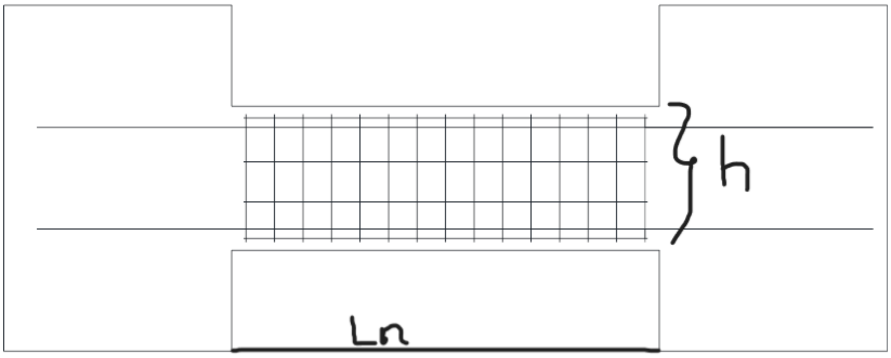

FIGURE 2.1: CONVENTIONALLY REINFORCED COUPLING BEAM.

To begin with, a scientist named Tom Paulay investigated the response of CRCBs with an aspect ratio of less than 1.5. The test results indicated that the beams with this reinforcement configuration did not behave as intended because they failed in the sliding shear. Additionally, the beams exhibited less ductile behaviour because they experienced a significant loss of strength when they approached the inelastic range (T.Paulay, 1969).Professor T. Paulay conducted additional testing on CRCBs in 1974 to assess their post-elastic performance (R.Park and T.Paulay, 1974). When the beams underwent several high-intensity load reversals, the tests showed three different ranges of behaviour. Figure.2.2 displays a replicated typical coupling beam's load-deformation curve.

Chapter 2: Previous Experimental Studies On Coupling Beams

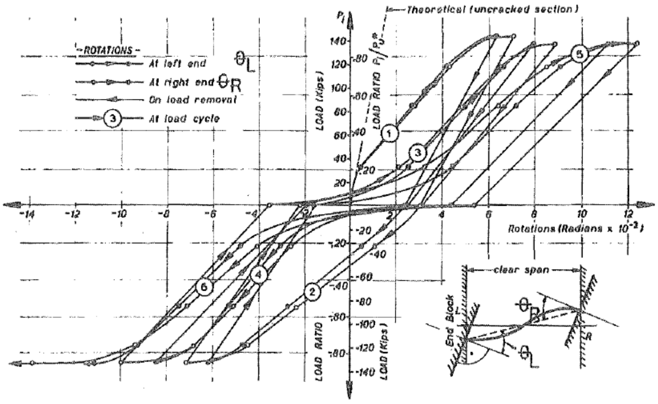

FIGURE 2.2: A TYPICAL LOAD-ROTATION CURVE OBSERVED BY PAULAY (1974) FOR CRCBS WITH ASPECT RATIO OF 1.29.

The rotations connected to the shear deformation of the stirrups and diagonal concrete struts are greater than the flexural deformation for the aspect ratio of the beam under examination (Ln/h=1.00) (Santhakumar, n.d.). According to the observations for beams with a span- to-depth ratio of less than 1.5, only 85% of the flexural strength was expected to develop based on conventional ultimate load analysis that would develop. Figure.2.3 illustrates the model that incorporates every member whose deformation causes conventional beams to rotate

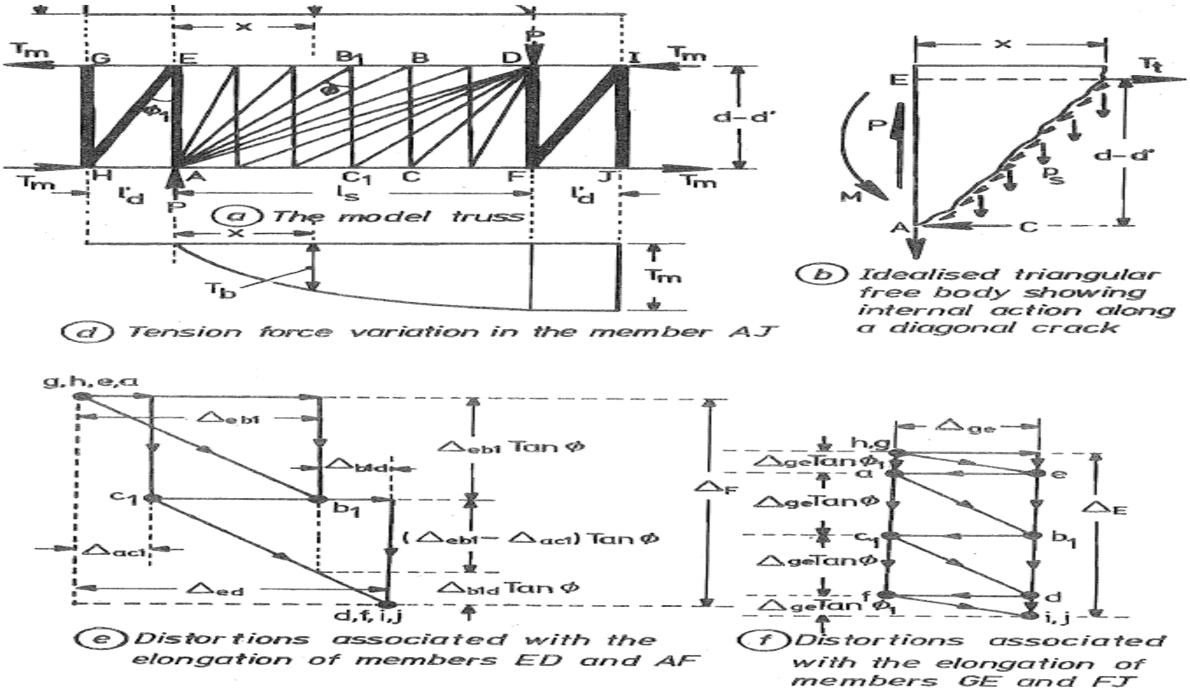

FIGURE 2.3: DISTORTIONS ASSOCIATED WITH THE ELONGATION OF THE TOP AND BOTTOM FLEXURAL BARS OF THE CONVENTIONALLY REINFORCED COUPLING BEAMS (SANTHAKUMAR).

Three conventionally reinforced beams were tested (Bhunia et al., 2013); the first two had an aspect ratio of 2.5 and the third had a ratio of 5.0. The test findings, which showed that all three beams failed in sliding shear and diagonal tension, were in line with those of Paulay. Additionally, the test results demonstrated that, in comparison to the other two beams with a 2.5 aspect ratio, the beam with a higher aspect ratio exhibited behaviour that is more ductile. Under cyclic loading, the CRCB fails in shear-sliding mode, as shown in Fig. 2.4 (Paulay, 2011). Intersecting flexural-shear cracks spread throughout the entire depth of the beam at its ends in this failure mode. Since the plane along which sliding develops is parallel to the transverse reinforcement, even tightly spaced stirrups lose their ability to transfer shear forces (Paulay, 2011).

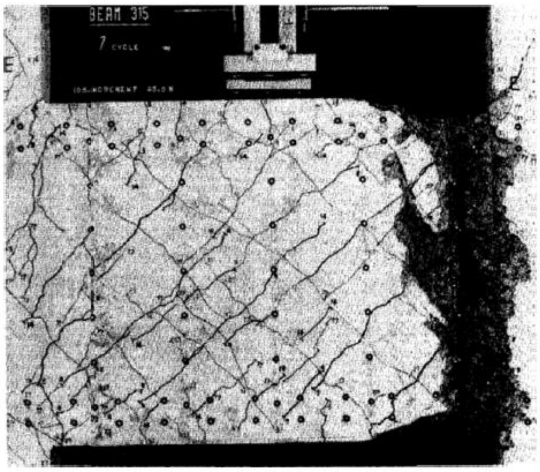

FIGURE 2.4: SLIDING SHEAR FAILURE IN COUPLING BEAMS (COURTESY TO PARK AND PAULAY 1975).

Tassios and the other scientists tested two conventionally reinforced coupling beams with aspect ratios of 1 and 1.66 to study the conventionally reinforced beams (T. Tassios, M. Moretti, A. Bezas, 1996). According to the test results, the beams failed in shear compression and diagonal tension, respectively. Compared to the beam with the lower aspect ratio, the one with the higher aspect ratio exhibited a more ductile behaviour. Six conventionally reinforced coupling beams with high-strength concrete were tested by Xiao and others (Yan Xiao, Asadollah Esmaeily-Ghasemabadi, and Hui Wu, 1999). Aspect ratio, primary reinforcement, and transverse reinforcement were the three main test variables. The test results demonstrated that the increased shear demand would cause the beam's ductility to decrease as the primary reinforcement ratio increased. Furthermore, the results corroborated the findings of Tassios and others, that the behaviour that is more ductile and less pinching were seen with an increase in aspect ratio. In conclusion, the findings indicated that raising the transverse reinforcement ratio would improve the beam's ductility and postpone the sliding shear failure.

A recently developed test technique that can properly replicate the boundary conditions of coupling beams in linked shear wall constructions was used to evaluate six half-scale models of reinforced concrete coupling beams with span/depth ratios < 2·0 under reversed cyclic stress. Only one was diagonally reinforced, while the other five were normally reinforced. The conventionally reinforced coupling beams exhibited a distinct behaviour from the regular beams in frame systems, as demonstrated by the test findings. Shear failure was often more likely to happen. The load-resisting mechanism was drastically altered and the coupling beam's ability to dissipate energy was greatly increased by the addition of diagonal reinforcement. It had not, however, increased the coupling beam's deformability (Kwan & Zhao, 2002). Four conventionally reinforced beams with varying aspect ratios, primary reinforcement ratios, and transverse reinforcement ratios were tested by Brena and Ihtiyar (Breña & Ihtiyar, 2011). In terms of the impact of aspect ratio, primary reinforcement ratio, and transverse reinforcement ratio, the test results agreed with those of earlier experiments. The behaviour of a single, conventionally reinforced beam with a 3.33 aspect ratio was examined (D. Naish, A. Fry, +1 author J. Wallace, 2013). The beam exhibited a suitable degree of ductility, and the results corroborated those of the previously tested beams, indicating that these beams could be employed in low shear stress demand areas with shear stress levels below $5\sqrt{f'c}$. Seo et al. (2017) ran an experiment on four traditionally reinforced beams with an identical aspect ratio of 1.68. To prevent sliding shear failure at the beam-wall interface, U-type reinforcement was added to the beams during fabrication and they were reinforced horizontally with anchors set into the walls. The test results demonstrated that adding reinforcement that was anchored into the wall would strengthen the beam. Because U-type reinforcement was used at the joints, the shear deformation concentrated in the middle of the beam, causing the beams to fail in shear.

Research on alternative reinforcement configurations has been prompted by concerns regarding the insufficient ductility of CRCBs. Thus, in the early 1970s, the concept of employing diagonal reinforcement to enhance beam behaviour was presented (Monthian Setkit, 2012, 2012; R.Park and T.Paulay, 1974; Santhakumar, n.d.)

2.3.3 Diagonally Reinforced Coupling Beams (DRCBs)

Paulay introduced a new reinforcement configuration aimed at preventing shear sliding failure, improving the coupling beams' response, and exhibiting more ductility (R.Park and T.Paulay, 1974). As seen in Figure 2.5, the new suggested reinforcement configuration was diagonally oriented reinforcement. These beams are known as diagonally reinforced coupling beams (DRCBs). The diagonal reinforcement was supposed to mimic the behaviour of cross bracing, with one bundle of bars under compression and the other bundle under tension, according to the theory behind the DRCBs' proposal. In general, diagonal steel can transfer the entire shear force in this reinforcement configuration (see Figure 2.5)(Monthian Setkit, 2012).

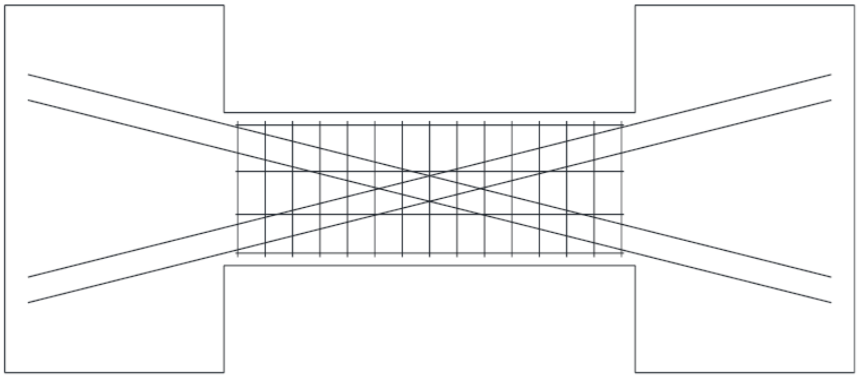

FIGURE 2.5 : DIAGONALLY REINFORCED COUPLING BEAM (MONTHIAN SETKIT, 2012).

The diagonal reinforcement design was based on the idea that steel forces alone could resist the shear and moment on the coupling beam (Santhakumar, n.d.). Uniformly stressed diagonal reinforcement that acts in tension along one diagonal and compression along the other provides this. The diagonal reinforcement's purpose is to provide a stable shear-resisting mechanism along the beam span and to stop a sliding shear failure. As long as sufficient lateral ties are supplied to allow the compression diagonal to sustain the yield load without buckling, the tests carried out by Paulay (T.Paulay, 1969) and later by Binney have demonstrated that these beams much more successfully meet the ductility demands indicated by the theoretical studies (Santhakumar thesis).

FIGURE 2.6: PROFESSOR TOM PAULAY WORKING ON THE DIAGONALLY REINFORCED COUPLING BEAM IN THE CORE WALL OF CHRIST CHURCH GENERAL HOSPITAL (COURTESY OF J.I.RESTREPO).

According to Penelis and Kappos (Bhunia et al., 2013), these coupling beam types have a better plastic rotation capacity than CRCBs during an earthquake when the aspect ratio is less than or equal to 1.5. They also have a minimum of four bars per diagonal. Three diagonally reinforced coupling beams were put to the test under cyclic loading by Pualay and Binney in 1974 (Paulay, 2011). The test results demonstrated that the new reinforcement configuration improved the beams' ductility, decreased their strength degradation, and stopped the slides from failing under shear, resulting in more desirable beam behaviour. The buckling of the compression bars caused the diagonally reinforced coupling beams to fail (Bahaa Ahmad Burhan Al-khateeb, 2021). A coupled wall with diagonally reinforced coupling beams was tested by Santhakumar (Santhakumar, n.d.). The findings corroborated those of Paulay and Binney (1974) since the diagonal arrangement of the reinforcement would improve the beams' ductility (Fig. 2.6).

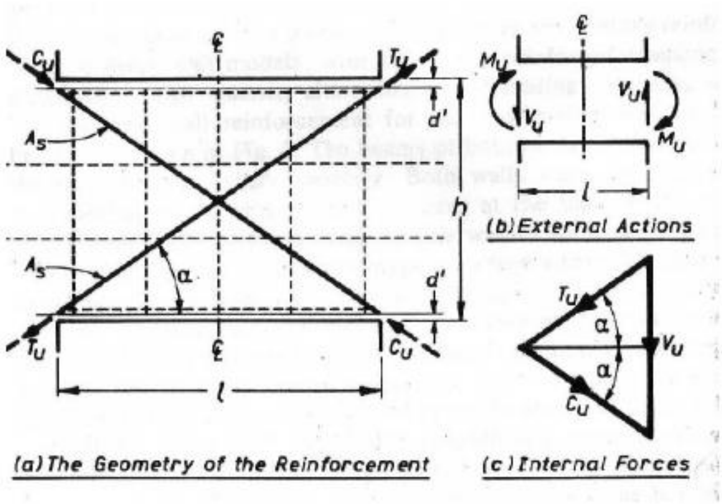

FIGURE 2.7: MECHANISM OF LOAD RESISTANCE IN A DIAGONALLY REINFORCED COUPLING BEAM (PAULAY AND SANTHAKUMAR 1976).

The response of two diagonally reinforced coupling beams with 2.5 and 5 aspect ratios was investigated by (Bahaa Ahmad Burhan Al-khateeb, 2021). According to the test results, the lower aspect ratio beams exhibited improved ductility, energy dissipation, and strength degradation. When compared to the beam with a shorter span, the diagonal reinforcement in the longer beam did not significantly improve the beam's ductility, energy dissipation, or strength degradation. Two diagonally reinforced coupling beams with aspect ratios of 1 and 1.66 were studied by Tassios and the others (T. Tassios, M. Moretti, A. Bezas, 1996). The beams' satisfactory ductile behaviour was demonstrated by the results. Kwan and Zhao examined a single coupling beam that was diagonally reinforced and the results indicated that the diagonally reinforced beam had improved energy dissipation, in line with earlier research(Kwan & Zhao, 2002). The goal of Fortney's experimental research from 2008 was to examine how the coupling beam behaviour is impacted by the transverse reinforcement ratio. Test results for two diagonally reinforced beams indicated that increasing the transverse reinforcement ratio would improve the beam's ductility and lessen its strength degradation (Fortney et al., 2006).

Conversely, if the transverse reinforcement ratio was increased, it would make the beam extremely crowded and challenging to build because it would be challenging to get concrete into the gaps between the steel bars. Therefore, building a beam with a lower transverse reinforcement ratio would be easier depending on the shear demand of the beam. To compare the effects of confining the entire section versus just the diagonal reinforcement bundle, Naish and other scientists tested seven diagonally reinforced coupling beams (D. Naish, A. Fry, +1 author J. Wallace, 2013). Additionally, the tests aimed to investigate the impact of a slab on the behaviour of the coupling beam. The test results demonstrated that, in comparison to beams with diagonal bundle confinement, the full-section confinement beam would exhibit improved ductility and strength degradation behaviour. Experimental testing was conducted on two diagonally reinforced concrete coupling beams with aspect ratios of 1.0 and 2.0 (Lim et al., 2016). The goal of the study was to suggest a new approach to diagonally reinforced beam design. According to the test results, a higher flexural strength could be achieved by designing the diagonally reinforced beams using the ACI 318-14 method (Monthian Setkit, 2012). Shear and moment capacities provided by the diagonal reinforcement can be determined as:

$$Tu = Cu = As.fy \qquad (1.32)$$

$$Vu = 2.Tu.sin\alpha = 2.As.fy.sin\alpha \qquad (1.33)$$

$$Mu = (As.fy.cos\alpha).\left(h-2d\right) \qquad (1.34)$$

Where: Tu and Cu stand for the diagonal reinforcement's ultimate tension and compression forces, respectively. Vu and Mu are the shear and moment, respectively, associated with the diagonal reinforcement yielding, h is the beam depth, α is the angle of the diagonal reinforcement concerning the beam longitudinal axis, and fy is the diagonal reinforcement yield strength.

The buckling of diagonal bars caused diagonally reinforced concrete coupling beams to fail. Consequently, it was suggested that transverse reinforcement be placed at regular intervals along the diagonal bars' length to prevent bar buckling at significant displacement reversals. Another testing program was carried out at the Portland Cement Association to investigate the behaviour of coupling beams under reversed cyclic loading. Three distinct reinforcement schemes were tested on eight reinforced concrete coupling beams. Three beams with a traditional reinforcement configuration made up the first set. Stirrups were made to withstand total shear, per Paulay's recommendation. Three beams in the second set had diagonal bars close to the interface between the beam and the wall. The entire shear force was intended to be supported by the diagonal reinforcement in the hinging region. The third set consisted of two beams with one bar in one direction and two bars in the other for full-length diagonal reinforcement. Tests were conducted with span-to-depth ratios of 2.5 and 5.0 for each type of detailing. Although it could prevent sliding shear failure, the diagonal reinforcement in the hinge region, also known as rhombic reinforcement did not considerably enhance the coupling beams' performance as was predicted (G.B Barney, K.N. Shiu, B.G.Rabbat and A.E.Fiorata, 1976).

The loss of efficient truss action resulted from the bent points of the diagonal bars because the concrete within the diagonal reinforcement region deteriorated by crushing and spalling as loading increased into the inelastic range (Monthian Setkit, 2012). Given the minimal enhancement in energy dissipation and stiffness retention, there was no need to increase the intricacy and construction expenses for this reinforcement arrangement. While diagonally reinforced coupling beams show good seismic behaviour, certain drawbacks are visible. Initially, the requirement for closely spaced transverse reinforcement around diagonal bars makes construction challenging. To prevent interference between diagonal bars at the mid-span of the beam, the diagonal cages are positioned in separate planes. This frequently results in a wider beam, which could mean bigger walls.

2.4 Different Reinforcement Configurations

Other than the conventional and diagonal layouts, several research projects investigated reinforcement configurations to determine their impact on the behaviour of the coupling beam to obtain the best coupling beam response in terms of ductility, energy dissipation, and strength. To prevent short coupling beams from collapsing in shear, Tegos and Penelis suggested setting up the primary reinforcements in a rhombic truss-like configuration with an inclination (I. A.

Tegos and G. Gr. Penelis, 1988). Twenty-four columns and coupling beams with aspect ratios between 2.0 and 5.0 were put to the test. Three specimens with diagonal reinforcements, three with only longitudinal and transverse reinforcement, and eighteen with inclined rhombic reinforcement were tested. The loadings used for the tests could be either cyclic or monotonic. An oil jack at one end of the specimen was used to apply axial load to the specimens, in contrast to other earlier research studies that did not take axial force into account (Monthian Setkit, 2012). The test results demonstrated that the rhombic reinforcement layout beams performed comparably to diagonally reinforced concrete beams in terms of performance. However, they did not directly compare energy dissipation, stiffness decay, or ultimate strength in their findings. The effect of a new reinforcement layout was examined and as seen in Figure 2.7, the beams had longitudinal bars spanning the length of the beam and diagonal reinforcement at the two ends of the beam, where plastic hinges are anticipated to occur (G.B Barney, K.N. Shiu, B.G.Rabbat and A.E.Fiorata, 1976).

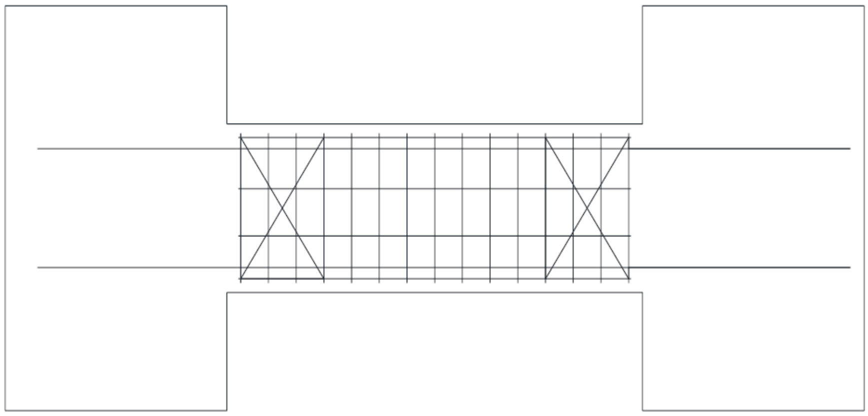

FIGURE 2.8: COUPLING BEAM REINFORCEMENT CONFIGURATION WITH DIAGONAL BARS AT THE LOCATIONS OF PLASTIC HINGES (MONTHIAN SETKIT, 2012).

Ten coupling beams were tested under cyclic loading as part of an experimental program, to assess the potential for alternative detailing (T. Tassios, M. Moretti, A. Bezas, 1996). These specimens had two distinct span-to-depth ratios (1.0 and 1.66) and five distinct reinforcement layouts, all at roughly half of the full scale. In Figure 2.8, the five reinforcement layouts are displayed. Following an investigation, the behaviours of three different reinforcement configurations (Figures 2.8 (c), (d), and (e)) were compared to those of conventionally and diagonally reinforced coupling beams (Figures 2.8 (a) and (b)).

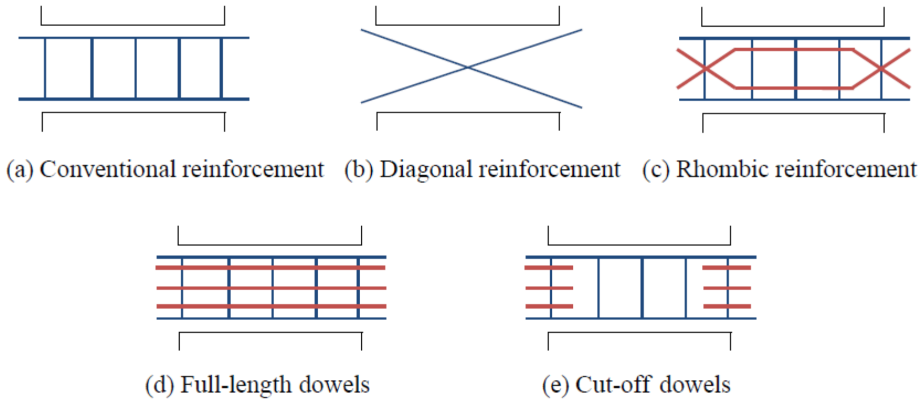

FIGURE 2.9 :REINFORCEMENT CONFIGURATIONS INVESTIGATED BY TASSIOS (MONTHIAN SETKIT, 2012)

Additional bent-up bars intersecting at the mid-height of the beam were used in the first detailing, known as a rhombic layout (Figure 2.4(c)). These bent-up bars increased the sliding resistance, but the flexural capacity at the beam-ends was not significantly increased. Long and short dowels were positioned across the ends of the beams in the second and third detailing (Figure 2.4(d) and 2.4(e)). The purpose of the dowel bars was to stop a sliding shear failure at the wall-beam interface. According to test results, the rhombic layout produced an overall better behaviour than the conventionally reinforced specimen (T. Tassios, M. Moretti, A. Bezas, 1996).

Comparing this reinforcement scheme to diagonally reinforced coupling beams, less intricate detailing is also needed. On the other hand, significant pinching of the hysteresis loops was noted, indicating a decrease in energy dissipation. It was discovered that dowel bars in the beam's end regions might aid in preventing a sliding shear failure in specimens that had them. Nonetheless, significant pinching and stiffness degradation were still seen in the hysteresis loops. The diagonally reinforced coupling beams performed the best in terms of energy dissipation and shear resistance, according to a comparison of hysteresis loops. In sum, for coupling beams with a span-to-depth ratio less than 2.0, diagonal reinforcement was still found to be the best solution (Monthian Setkit, 2012).

A report on the testing of fifteen short coupling beams was published by Galano and Vignoli (Luciano Galano and Andrea Vignoli, 2000). There were four distinct reinforcement configurations tested. They were as follows: (a) traditional layout (conventional reinforcement); (b) diagonal layout without ties that confine; (c) diagonal layout with ties that confine); and (d) rhombic layout with inclined bars. The span-to-depth ratio for each specimen was 1.5. According to test results, beams with rhombic or diagonal reinforcement detailing performed better than those with a traditional reinforcement layout. There was very little difference in the dissipation of energy between the rhombic and diagonal layouts. When compared to diagonal layouts, the rhombic layout offered greater advantages in terms of strength retention and rotational ductility capacity. This assertion runs counter to Tassios and others' findings (Monthian Setkit, 2012).

2.5 Conclusion

The results of the tests showed that all tested specimens could develop flexural yielding before the beams failed due to sliding shear. The coupling beams with distributed flexural reinforcement showed significantly better hysteretic response and ductility when compared to the coupling beams with conventional reinforcement. Diagonal reinforcement greatly enhances ductility, stiffness retention, and energy dissipation in coupling beams, according to experimental studies (G.B Barney, K.N. Shiu, B.G.Rabbat and A.E.Fiorata, 1976; Luciano Galano and Andrea Vignoli, 2000; Paulay, 2011; T. Tassios, M. Moretti, A. Bezas, 1996; T.Paulay, 1969). Other reinforcement detailing, like the different rhombic configurations that were proposed, demonstrated inadequate seismic behaviour and presented significant construction challenges.

Chapter 3: Finite Element Analysis of Conventionally Reinforced Concrete Short Coupling Beam

3.1 Introduction

This chapter discussed the application of finite element analysis to the solution of the conventionally reinforced concrete short coupling beam with an aspect ratio of two ($\frac{Ln}{h} = 2$). For simulating the behaviour of the short coupling beam specimen, material models and underlying assumptions were determined by numerical modelling with the finite element software (Cast3m). The parametric assessments of short coupling beams subsequently made use of this model and presumptions. In Section 3.2, a succinct presentation of Cast3m software is illustrated. Moreover, Section 3.3 presents actual numerical protocols about the reference experimental findings. Boundary conditions, material models, and model limits are the main topics of discussion. As described in Section 3.4, the CRCCB, which has an aspect ratio of two, has the calculated shear stress of $0.33\sqrt{f'c}$. The actual finite element modelling of the short CRCCB is demonstrated in Section 3.5. The test results, reactions to the load-displacement and the shear strength analysis are provided in the sections that follow.

3.2 Brief Presentation of Cast3m Software

The software called Cast3M ex-Castem2000 is used to compute structures using the finite element method and, more generally, to solve partial differential equations using the finite element method. The Department of Mechanics and Technology (DMT) of the Atomic Energy Commission (CEA) developed this software.Cast3m 2000's primary unique feature is its exceptional adaptability to the various applications that are unique to each user. Castem2000 has been available for free use in education and research since the summer of 1999. Developers can also access the source code and in 2001, Castem2000 became cast3M. For more information consult the site, where you will find the software for free download and the documentation: (http://www-cast3m.cea.fr). The finite element method splits the coupling beam into multiple smaller elements using the Cast3m programming language.

3.3 Test Setup, Instrumentation, and Loading Protocol

For this investigation, a nonlinear finite element model was developed and calibrated from experimental coupling beam test data provided by previous researchers (Sesli & Husem, 2021). Following the Turkish Earthquake Code 2018 and ACI 318-14, which were used in the design of conventionally reinforced concrete coupling beam (CRCCB) and diagonally reinforced coupling beam with fully confined concrete section (DRCCB-FC), only the equations for calculating shear strength were applied. To expedite the numerical analysis, the shear wall piers in this research were modelled to only behave elastically; however, the short coupling beams were treated under a post-elastic state.

Consequently, the model was supported with a double articulation at one end of the wall pier and with simple support at the other end, to maintain the isostatic state of the wall system. Both the numerical and the experimental research ignored the vertical load on the shear wall piers. The CRCCB analysed in this research used similar procedures, beam dimensions, and geometry to assess and contrast computed results with the provided experimental evidence. For comparison reasons, the simulated CRCCB was analysed under static loading and using the quasi-static displacement-controlled cyclic loading history outlined in FEMA-461 Chapter 2.9.1 (Appplied Technology Council, 2007).The following figure displays the quasi-cyclic loading trajectory.

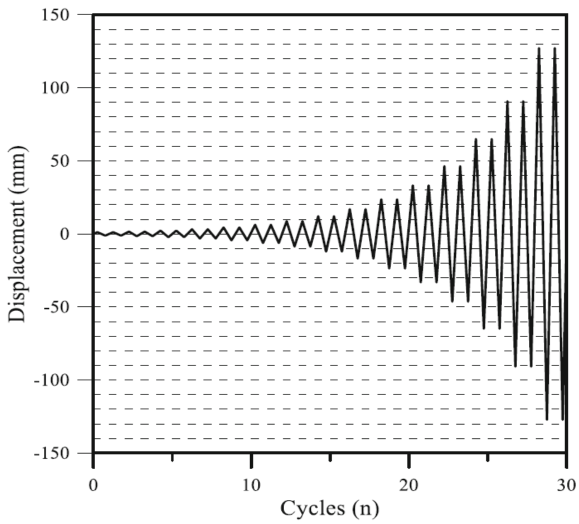

FIG.3.1 PHASE-BY-PHASE DISPLACEMENT-REGULATED CYCLIC LOADING TRAJECTORY (SESLI & HUSEM, 2021).

3.4 Specimen Dimensions and Reinforcement Configuration

When coupling beams have a calculated shear force Vu greater than $0.33\sqrt{f}'c.Acw$ and an aspect ratio of (ln/h)≥ 2, where [Acw = area of concrete section and f'c=specified compressive strength of concrete]. The ACI 318–14 states that coupling beams may be strengthened using traditional reinforcement (conventional reinforcement) (*Building Code Requirements for Structural Concrete (ACI 318-14) [and] Commentary on Building Code Requirements for Structural Concrete (ACI 318R-14),* 2014). The aspect ratio of two

($\frac{Ln}{h} = 2$), conventional reinforcement and calculated shear stress of $0.33\sqrt{f'c}.Acw$ were the design criteria; the importance of the transverse reinforcing bars and concrete was not considered in the numerical work and in the experimental work (Sesli & Husem, 2021). The coupling beam's clear span and depth were 900 mm and 450 mm, respectively, hence the selected aspect ratio was two. The conventionally reinforced coupling beams' size and reinforcing details are displayed in Fig. 3.3.

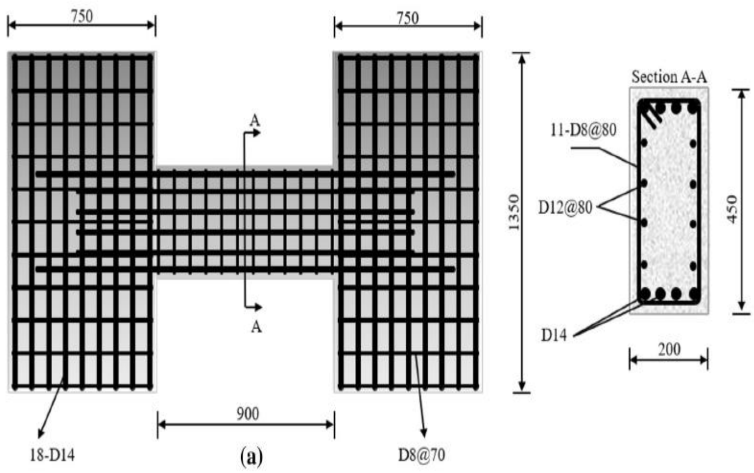

FIGURE 3.2: DIMENSIONS AND REINFORCEMENT DETAILS OF CONVENTIONALLY REINFORCED COUPLING BEAM SPECIMEN: (CRCCB)(SESLI & HUSEM, 2021).

Since the transverse reinforcement, spacing (D8) cannot be larger than six times the diagonal bar diameter, as per ACI 318-14, it was 80 mm. Concrete with a notional 28-day compressive strength (f'c) of 25MPa and steel bars with a nominal yield strength (f y) of 420 MPa were used to create the numerical test specimen. According to Kwan and Zhao, the wall piers have to be planned with a width bigger than the beam depth and a height bigger than twice the beam depth (Kwan & Zhao, 2002). As a result, the wall piers in our investigation were 750 mm wide and 1350 mm high (Sesli & Husem, 2021). The wall piers were designed with transverse reinforcement spaced 70 mm apart to yield a calculated shear stress value Vu of around $0.55\sqrt{f'c}$.

TABLE 1: CONVENTIONALLY REINFORCED CONCRETE SHORT COUPLING BEAM SPECIMEN-GEOMETRY

Specimen	Width b (mm)	Depth h(m)	Clear-Span Ln (mm)	Bar-Inclination Angle (^{o})	Diagonal Reinforcement	Horizontal Reinforcement	Transverse Reinforcement
					Diameter(mm)	Diameter(mm)	Diameter (mm)
CRCB	200	450	900	0.00	-	12-14	8

TABLE 2: SPACING, CONCRETE AND STEEL STRENGTH OF CONVENTIONALLY REINFORCED SHORT COUPLING BEAM SPECIMEN

Specimen	Spacing (mm)	Concrete Compressive Strength (FCB) MPa	Fracture Energy (GF) MPa	Tensile Strength of Rebar FTB(MPa)
CRCB	80	25	60	2

3.5 Finite Element Modelling of CRCB using Cast3m

The conventionally reinforced coupled beam specimens' behaviour was simulated using numerical models with the finite element software (Cast3m). This process aimed to ascertain the material models and assumptions that were required. The model and these presumptions were used for parametric assessments of coupled beams. The models' capacity to accurately replicate the flexural and shear behaviour of the coupling beams was then assessed by comparing the numerical results with the findings of the experimental tests. Figure 3.3

illustrates the mesh CRCB in Cast3m and Figure 3.4 displays the reinforcing detail of the CRCB under cyclic loading.

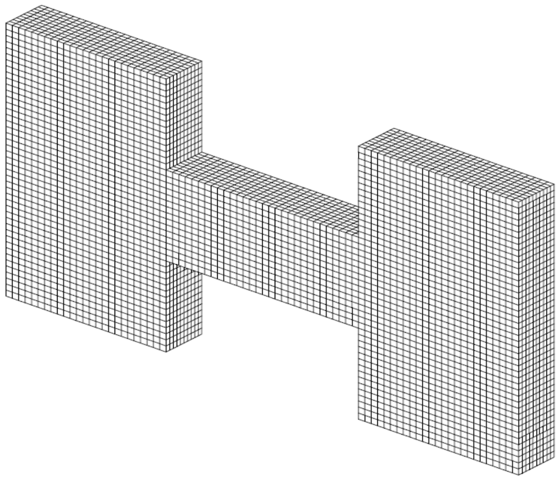

FIG.3.3: MESH OF THE FINITE-ELEMENT MODEL OF CRCCB

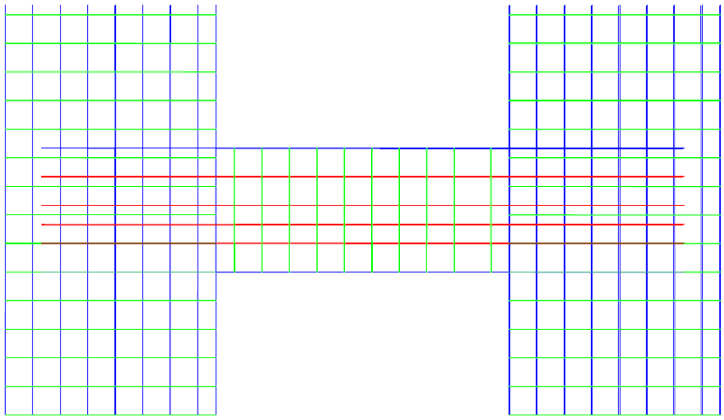

FIG.3.4: REINFORCEMENT OF CRCCB

3.6 Nonlinear Analysis of CRCCB specimen

The following Figures depict the formation and spread of concrete cracks, both in tension and compression zones. Under static loading, Figure 3.6 encapsulated moderate diagonal cracks, which developed at the middle of the beam, which proved the yielding of steel reinforcement due to excess stresses that outdid the yield strength. This signified the conception of plastic deformation in the beam specimen. The vertical fractures were a result of bending moments, which demonstrated flexural failure of the CRCCB specimen. The gradual rise of the bending moments in the beam's cross-section produced compressive and tensile stresses, which when they surpassed the yielding stress, led to plastic deflections. Additionally, at the beam-wall joints, few fissures were observed, this was because of the presence of plastic hinges.

By visually comparing the numerical and experimental findings, it was possible to determine that the crack-opening modes were identical (see Figure 3.6). Along through-depth flexural fractures in plastic hinge areas, shear sliding took place. In this beam specimen, longitudinal strains changed almost linearly as the cross section's depth increased. This supports the application of Bernoulli's theory that following loading, plane parts stay plane. In these figures, tensile strains are positive (see Figures 3.4 and 3.5). For our CRCCB specimen, the yielding drift was 0.49% and the maximum ultimate drift 0.80%. The yielding and maximum drift ratio were determined using the following equations:

$$\theta y = \frac{\partial y}{hw} \qquad (1.35)$$

$$\theta u = \frac{\partial u}{hw} \qquad (1.36)$$

Where: θy and θu are the yielding and maximum drift ratios respectively and hw represents the height of the wall pier.

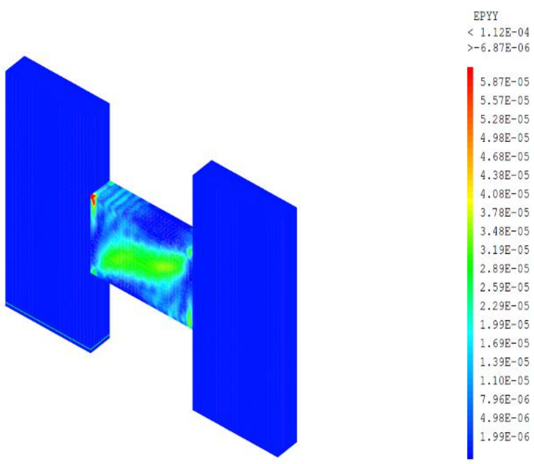

FIG.3.5: FAILURE MODE OF CRCCB UNDER STATIC LOADING.

A significant factor in the behaviour of conventionally reinforced short coupling beams is flexure. The accompanying figure (see Fig.3.6) accurately depicts the flexural failure and shear failure of the simulated CRCCB. The orthogonal double diagonal cracks developed across the beam section were a result of shear failure, caused complete collapse of the concrete core. Due to the presence of plastic hinges at the beam-wall interface, minimum cracks were developed. Concrete crushed in the compression zone where it reached its crushing state, which led to a fragile mode. The rebar fractured after reaching their yield point due to continuous cyclic loading and the capacity to carry/resist loads suddenly dropped. This shows that the CRCCB underwent ultimate load failure due to repeated reversed loads subjected to it.

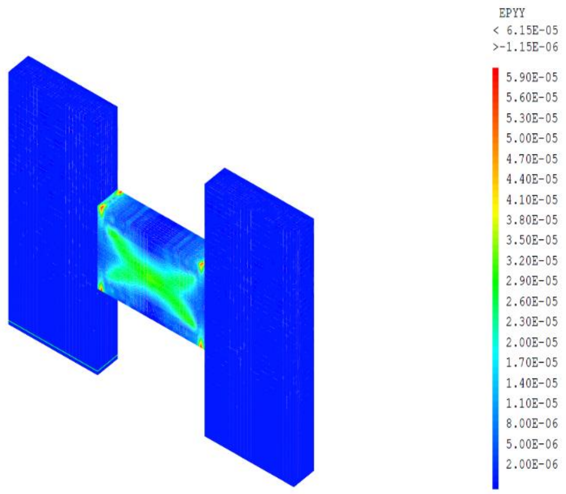

Fig.3.6: Failure mode of CRCB under quasi-cyclic loading.

In the following Figures 3.7(a) and (b), the numerical and experimental evidence showed that CRCCB specimens experienced diagonal splitting failure. Concrete, which is poor in tension led to the formation of cracks as its tensile yield strength, was exceeded. After the diagonal tension failure seen from the CRCCB specimen subjected to static loading (see Figure 3.5), cyclic loading sequence was performed, and the concrete in the CRCCB specimen's was predicted to crush and spall at the beam’s mid-span (see Fig.3.7). The CRCCB specimen gradually succumbed shear strength under cyclic loading as the specimen experienced diagonal tension failure.

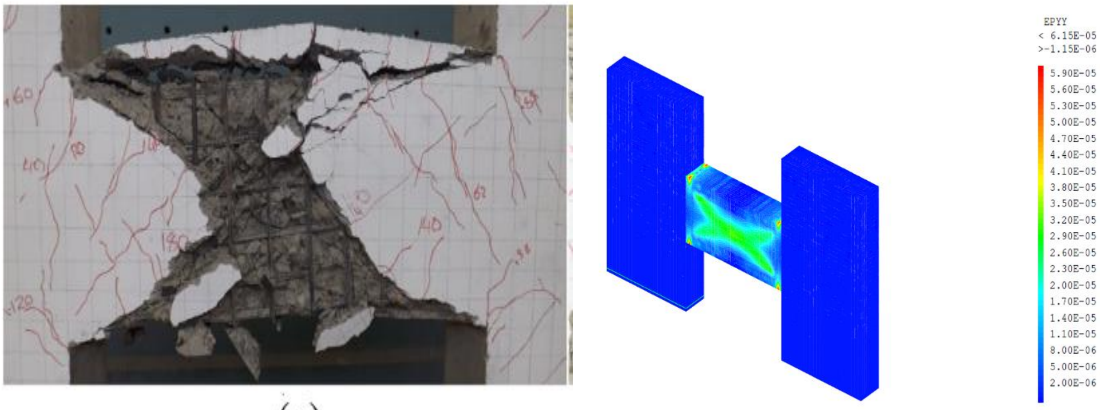

(a)

(b)

*FIG.3.7: (**A**)THE CONDITION OF EXPERIMENTAL CRCB SPECIMEN AFTER FAILURE (SESLI & HUSEM, 2021); (**B**)THE CONDITION OF NUMERICAL CRCCB MODEL AFTER FAILURE.*

3.7 Response to Load-Displacement

Figures 3.8 displays the specimens' load-displacement responses to lateral static load. From the graph, the peak load was 440KN. After reaching its ultimate load, the curvature became nonlinear, which marked the creation of a plastic hinge. There are three well defined ductility metrics, these include: cumulative, energy, and static ductility,(Sesli & Husem, 2021). The following equation (1.37) was applied to estimate the static ductility.

$$\mu = \frac{\partial u}{\partial y} \qquad (1.38)$$

Where ∂y the drift ratio at yielding and ∂u is the maximum drift ratio.

According to FEMA 306 the ductility capability is categorized as high for $u > 5$, moderate for$2 \leq u \leq 5$ and low for u <2 (Sesli & Husem, 2021).

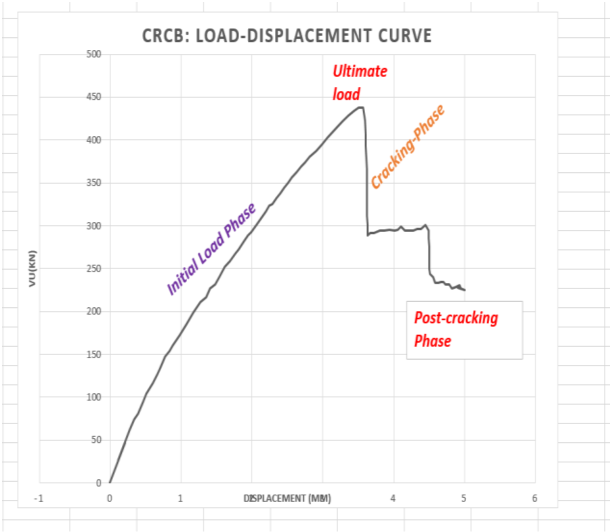

FIG.3.8: CRCCB: LOAD-DISPLACEMENT CURVE UNDER STATIC LOADING.

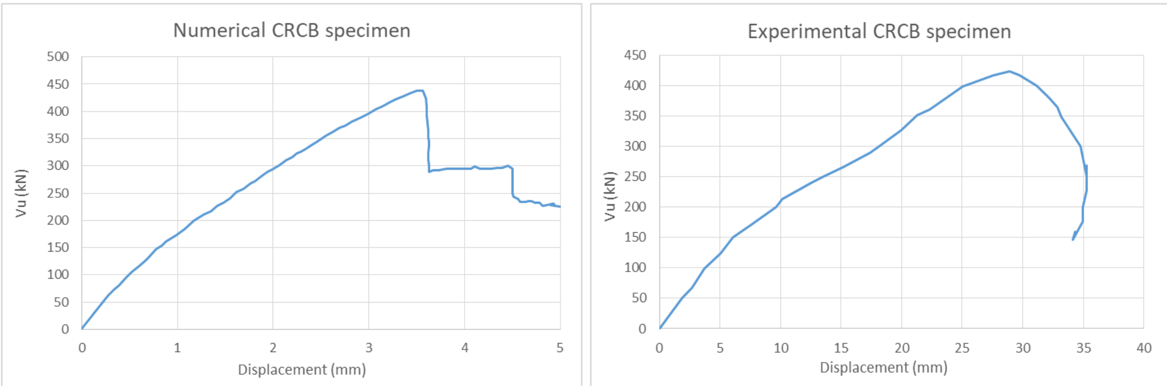

FIG.3.9: NUMERICAL AND EXPERIMENTAL BILINEAR CURVES FOR CRCB.

The repeated cyclic loading as encountered during seismic actions (earthquakes loads), caused accumulating damage and continuous yielding, which resulted in the making of plastic hinges in some points. Moreover, these plastic hinges resulted due to the fatigue experienced by specimen material. The following figure (see Fig.3.10) fully displays the results obtained after cyclic loading executions.

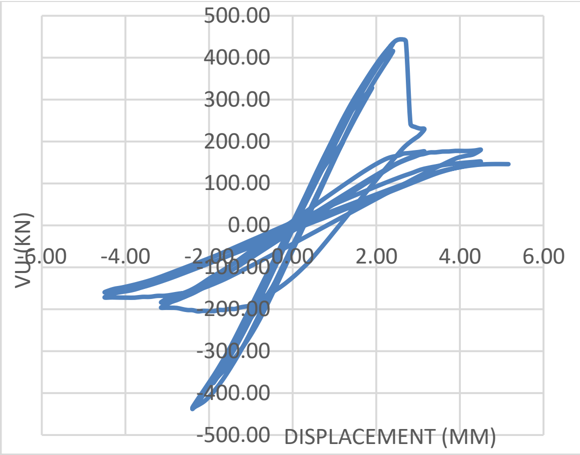

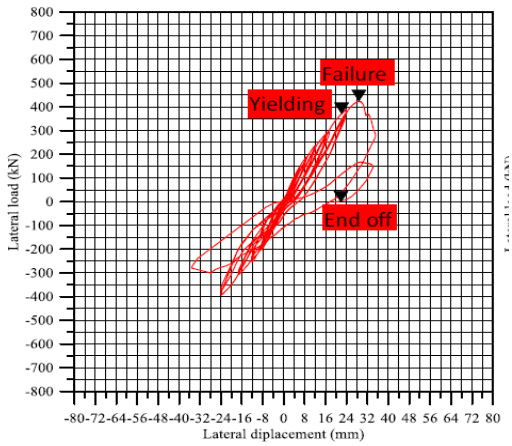

FIG.3.10: LOAD-DISPLACEMENT CURVE OF CRCCB UNDER CYCLIC LOADING (SESLI&HUSEM, 2021).

The location of the inflexion point was at the beam' mid-span (see Fig.3.11). At this point, the CRCB specimen, for a brief moment has no curvature, thus the bending moment is zero.

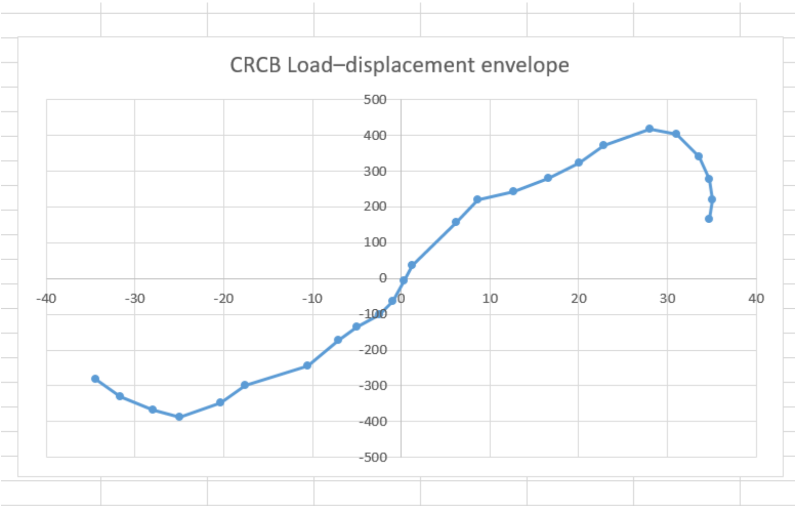

FIG.3.11: CRCCB LOAD-DISPLACEMENT ENVELOPE.

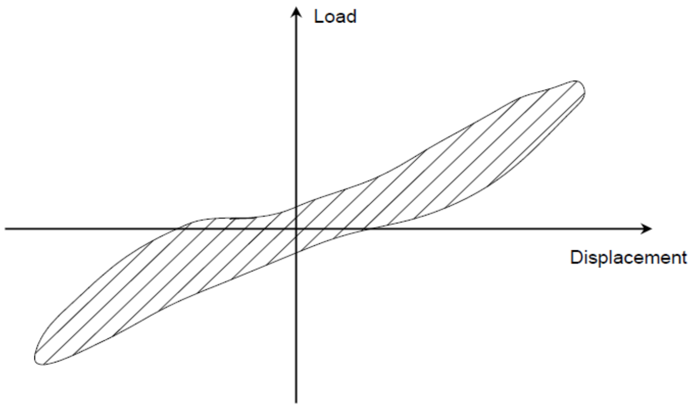

FIG.3.12: AN ANALOGOUS ELASTO-PLASTIC SYSTEM.

3.8 Shear Strength Analysis

Generally speaking, five main ways in which reinforced concrete members resist shear: shear that is carried by transverse reinforcement through truss action, shear that is resisted by the member compression zone, aggregate interlock, dowel action by the longitudinal reinforcement, and shear resistance from diagonal reinforcement (Monthian Setkit, 2012).

The design parameter in this work was an estimated shear stress (Vu):

$$Vu = 0.33.\sqrt{f'c}.Acw \quad (1.39)$$

However, both the transverse reinforcement and the concrete are capable of enhancing the shear strength (Sesli&Husem, 2021). For this reason, beams rather than shear walls were deliberately coupled using the method described in ACI 318-14 (Chapter 18).The conventionally reinforced coupling beam under diagonal stress has its shear strength (Vn) calculated using the following equation as per ACI 318-14.

(Section 18.10.4.1 in Chapter 18):

$$Vn = Acv.(\alpha c.\sqrt{f'c} + \rho.fy \quad (1.40)$$

Where: Acv = gross area of a concrete section limited by the section's length and web thickness in the direction of the shear force taken into consideration for walls;

αc = coefficient that indicates how much concrete strength contributes to the nominal wall shear strength. In this case αc= 0.17 (using 2 for inch) for$\frac{Ln}{h} > 2$. ρ = ratio of the gross concrete area perpendicular to the dispersed transverse reinforcement to its area (transverse reinforcement content).According to the Turkish Earthquake Code 2018, the factored shear strength of CRCB is calculated using the following equation:

$Vu = 1.5.b.h.fct$ (1.41)

The same equations provided in Chapter 1 of this study, for calculating shear strength according to Euro-code8 and RPA99/V2003 were applied in the same manner. To delineate the remarks from both numerical and experimental test results, calculations according to international standard codes were made (see Table 3).

TABLE 3.1: SHEAR STRENGTH RESULTS

Numerical Shear Strength	Vu= 440 KN
Experimental Shear Strength	Vu= 423 KN
Factored Shear Strength (Vu=0.33$\sqrt{f'c}.Acw$)	Vu= 148.5 KN

TABLE.3.2: THEORETICAL SHEAR STRENGTH

International Standard Code	**Theoretical Shear strength (KN)**
ACI 318-14	Vn =390 KN
Turkish Earthquake Code 2018	Vt = 337.5KN
EC8	VEd= 225KN
RPA 99/V2003	τb =185 KN

The following figure displays (see Fig.3.15) all the shear strength results drawn from the data and calculations. According to Figure 3.15, the highest shear strength resulted from the equation provided by ACI 318-14. This was because the code stated that for CRCB with an aspect ratio equal to two, the wall boundary was interpreted as being a column. Therefore, the equation used was for wall piers. The calculated shear strength according to international standard codes was different because of the safety and legal considerations. In addition to that, different countries have different seismic design codes, depending on geographical seismic zones, seismic activity, geology, building topology, cultural preferences, etc.

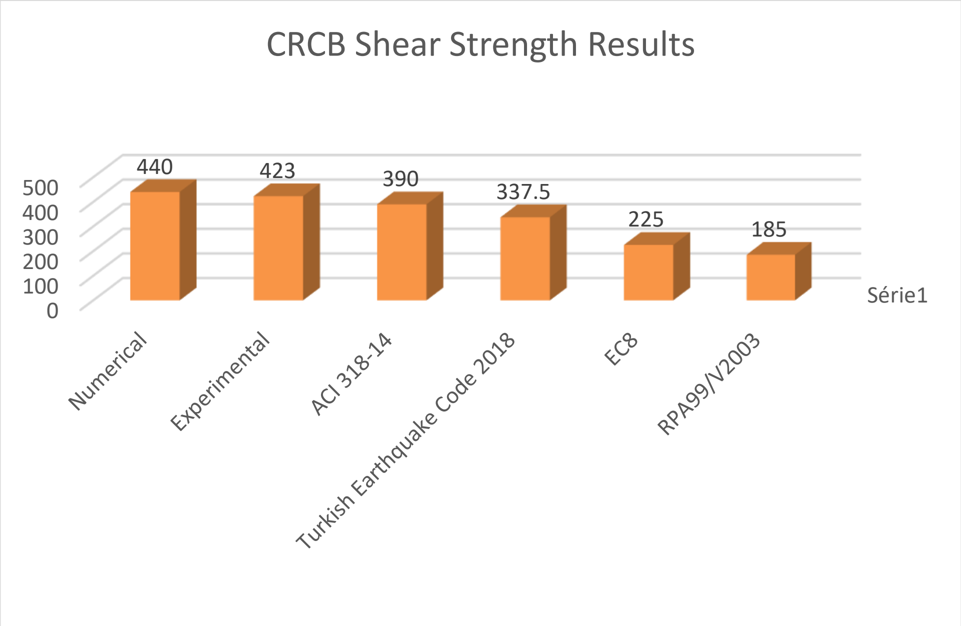

FIG.3.13 CRCB SHEAR STRENGTH RESULTS

The junction point of a line drawn from the origin to a point of ¾ of the ultimate load and a horizontal line at the ultimate strength is known as the drift ratio at yielding (∂y), it conform to the value given from lowering the strength to 0.75 times (Luciano Galano and Andrea Vignoli, 2000). As shown in Fig.3.20, the highest drift ratio (∂u) corresponds to a point at which the strength is lowered to 0.85 times the peak load. Transverse reinforcing bars and concrete both contributed to the shear strength in this investigation, but the calculated shear stress of (Vu=0.33$\sqrt{f'c}$ =1.65 MPa) was taken into account as a design parameter, ignoring their contributions in the design shear stress. The numerical ductility according to Fig.320 is 1.60 ($u = \frac{\partial u}{\partial y} = 1.60$) and as mentioned in FEMA 306, this ductility's capability is low ($u < 2$).

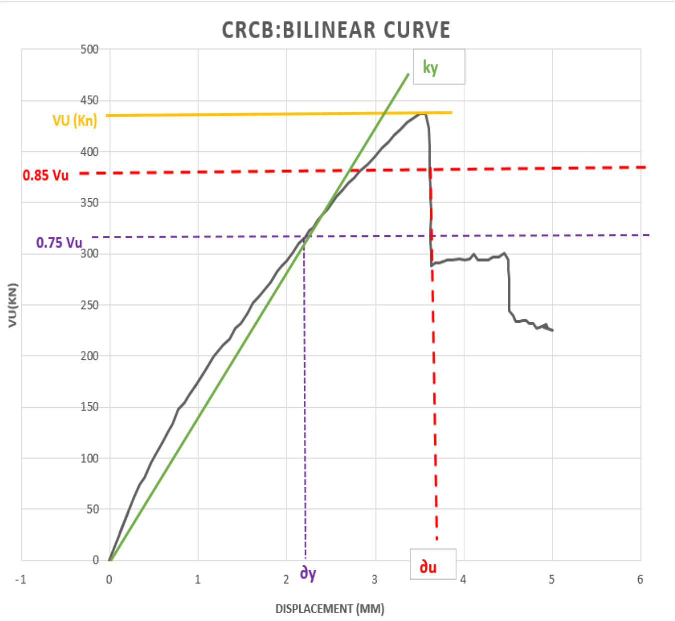

FIG.3.14: DEFINITION OF DUCTILITY ON LOAD-DISPLACEMENT ENVELOPE CURVE.

TABLE 3.3: SUMMARY OF CRCCB RESULTS

SPECIMEN	VU	VN ACI318-19	∂U	∂Y	ΘU	ΘY	U
NUMERICAL SPECIMEN	440 KN	390 KN	3.61	2.25	0.80%	0.49%	1.60
EXPERIMENTAL SPECIMEN	423 KN	376 KN	2.04	1.53	2.04%	1.53%	1.33

3.9 Conclusion

The simulated short conventionally reinforced coupling beam resulted in shear strength almost equal to the experimental one. Due to the steel lateral beam used in the loading of the experimental model, the numerical CRCCB experienced a shift in displacement values because of the lack of the steel beam. From the observations, the modelled CRCCB presented a low ductility meaning it could not deform after exceeding its yield point. Therefore, it could be predicted that the CRCCB cannot ensure a good post elastic behaviour. In conclusion, the simulated short coupling beam showed that conventional reinforcing was not particularly efficient in resisting shear forces; it failed in the shear mode due to repeated cyclic loads.

CHAPTER 4: Numerical Analysis of Diagonally Reinforced Short Coupling Beam

4.1 Introduction

This chapter is a continuous assessment of the finite element analysis of short coupling beams. In this case, a diagonally reinforced with full section-concrete short coupling beam (DRCB-FC) was analysed nonlinearly using Cast3m software. Section 4.1 demonstrates the numerical modelling procedures done on the DRCB-FC specimen. The cracking mechanism of the beam specimen was discussed in Section 4.2. In Section 4.3, the load-displacement response was revealed and the test results were interpreted. The DRCB-FC's shear strength observations were given in Section 4.4. Lastly, the data analysed in this chapter was summarised in the conclusion.

4.2 Numerical Modelling of the DRCB-FC specimen using Cast3m

The modelling procedure for the DRCB-FC was done considering the same aspect ratio ($\frac{Ln}{h}$=2), and the same dimensions as the previous CRCB specimen (see Chapter 3), but with a different reinforcing configuration. Based on the concrete cover and transverse reinforcement, the diagonal reinforcement inclination angle for diagonally reinforced specimens was 18.66 º. The initial implementation of a fully restricted section and diagonal reinforcement (DRCB-FC) of this research was designed following the ACI 318-14 and the Turkish Earthquake Code 2018. The following figure (see Figure 4.1) displays the actual numerical specimen of the DRCB-FC modelled using Cast3m software, presenting the longitudinal, transverse and the diagonal reinforcements. Moreover, Fig. 4.2 illustrates the geometry and the reinforcement configuration of the DRCB-FC used in this study.

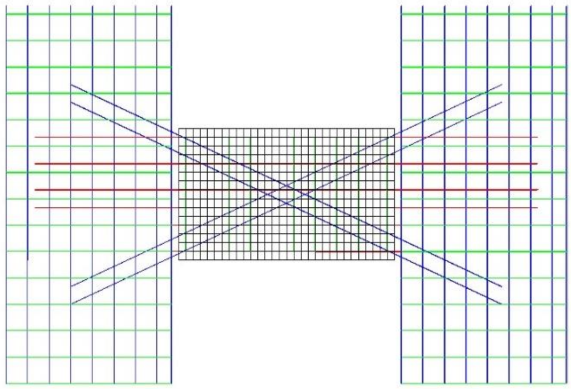

FIG.4.2: CAST3M DRCB-FC SPECIMEN

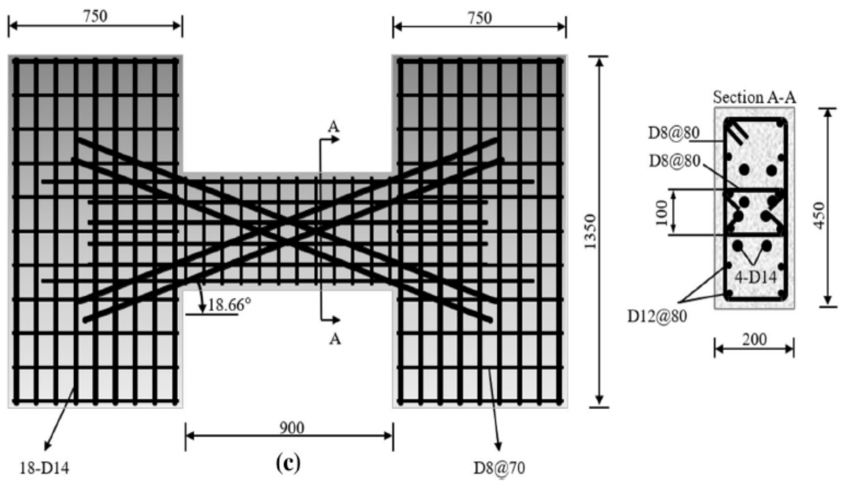

FIG.4.3: EXPERIMENTAL SPECIMEN OF DIAGONAL REINFORCEMENT WITH FULL CONFINED SECTION (DRCB-FC).

TABLE 4.1: DRCB-FC SPECIMEN GEOMETRY

Specimen	Width b (mm)	Depth h(m)	Clear-Span Ln (mm)	Bar-Inclination Angle (^{o})	Diagonal Reinforcement	Horizontal Reinforcement Diameter (mm)	Transverse Reinforcement Diameter (mm)
DRCB-FC	200	450	900	18.66	14	12	8

TABLE 4.2: DRCB-FC SPECIMEN CONCRETE AND STEEL PROPERTIES

Specimen	Spacing (mm)	Concrete Strength (f'c) MPa	Fracture Energy GF (MPa)	Tensile Strength (MPa)
DRCB	80	25	60	2.5

4.3 Crack operation of the DRCB-FC specimen

The nonlinear finite element technique was used to judge the cracking mechanism of the DRCB-specimen. The diagonally reinforced short coupling beam of this study was scrutinized under both static and cyclic loading to acknowledge how cracks commence, generate and affect global behaviour of the beam. The development and spread of cracks on the specimen are shown in the accompanying Figures. Due to tensile stresses, which are a result of bending, cracks in concrete are propagated (tension cracks) close to the beam-ends. Continuous loading (cyclic loading) give rise to shear stresses which when they overtake the beam's shear strength will result in diagonal cracks (see Fig.4.5). Although the presence of diagonal reinforcement aids in absorbing these shear stresses, addition of more shear forces will result in loss of the beam's shear capacity. The diagonal bars' role is to primarily carry the shear and tensile forces to limit crack opening in concrete, therefore in this DRCB-FC specimen moderate cracks are predicted on the concrete. Yielding of the diagonal bars give rise to the creation of plastic hinges that contribute in plastic deformation of the beam. The presence of plastic hinges allows for the repartition of the stresses, which aids in avoiding unexpected collapses and enhance the beam's ability to dissipate energy. Concrete is expected to crush in the presence of extremely large loads especially in the compression regions. In the DRCB-FC specimen, the rebar will fail due to buckling or it will rupture due to reduction of the loading-carrying capability. The software results makes it easier to visualize the cracks patterns (see Figures 4.5 and 4.6).

According to the numerical results, a few vertical fissures were seen at the stress corners, especially after running the analysis under the cyclic load. The DRCB-FC specimen expressed a single diagonal crack along the beam's cross-section due to cyclic loading. It is not possible to completely prevent or eliminate sliding shear failure at the contact between the wall and the beam especially when the beam is subjected to cyclic loading. Due to this failure mechanism, linked shear walls' ductility requirement was insufficient. As the aspect ratio and shear strength grow over the coupling beam span, Brena and Ihtiyar predicted that shear-sliding behaviour will occur in diagonally reinforced coupling beams (Breña & Ihtiyar, 2011). Since the shear wall piers in this study were only meant to exhibit elastic behaviour, the numerical findings did not reveal any notable shear fractures or wall pier damage.

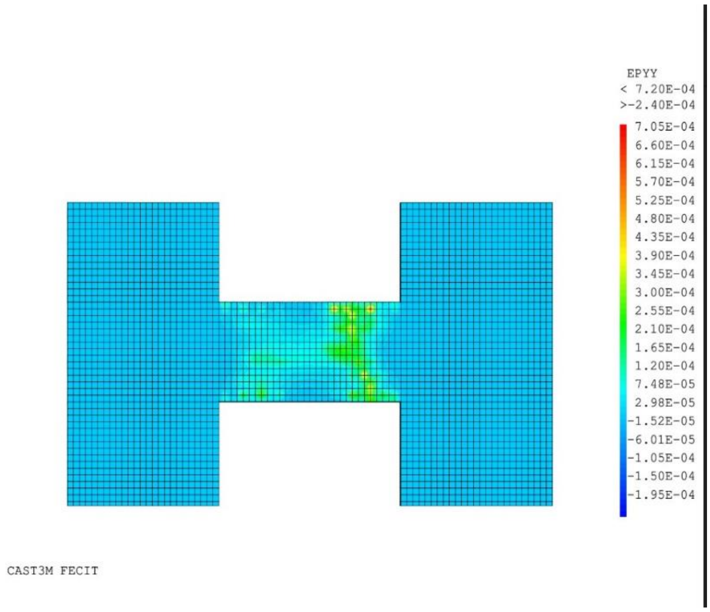

FIG.4.4: DRCB-FC CRACKING MECHANISM UNDER STATIC LOADING.

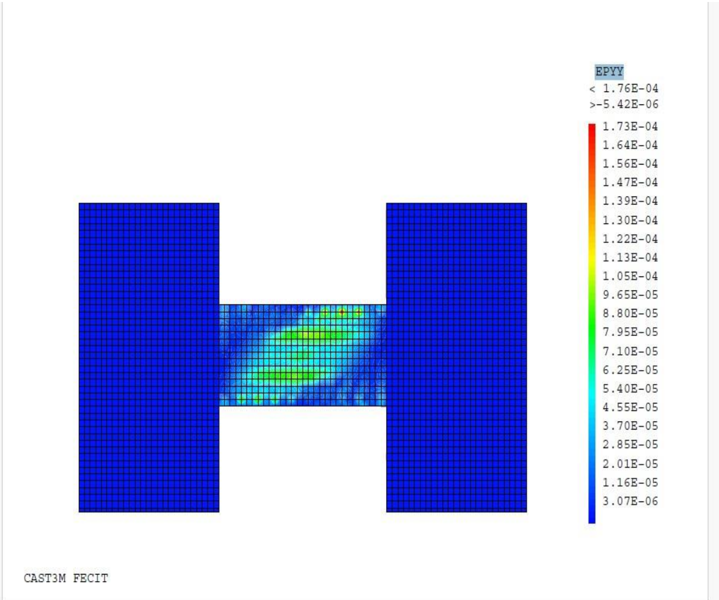

FIG.4.5: DRCB-FC CRACKING MECHANISM UNDER CYCLIC LOADING.

4.4 DRCB-FC's Load-Displacement Curves

Fig. 4.6 displays the specimen's load-displacement responses to lateral cyclic stress. The ultimate load of this beam was at 596KN.

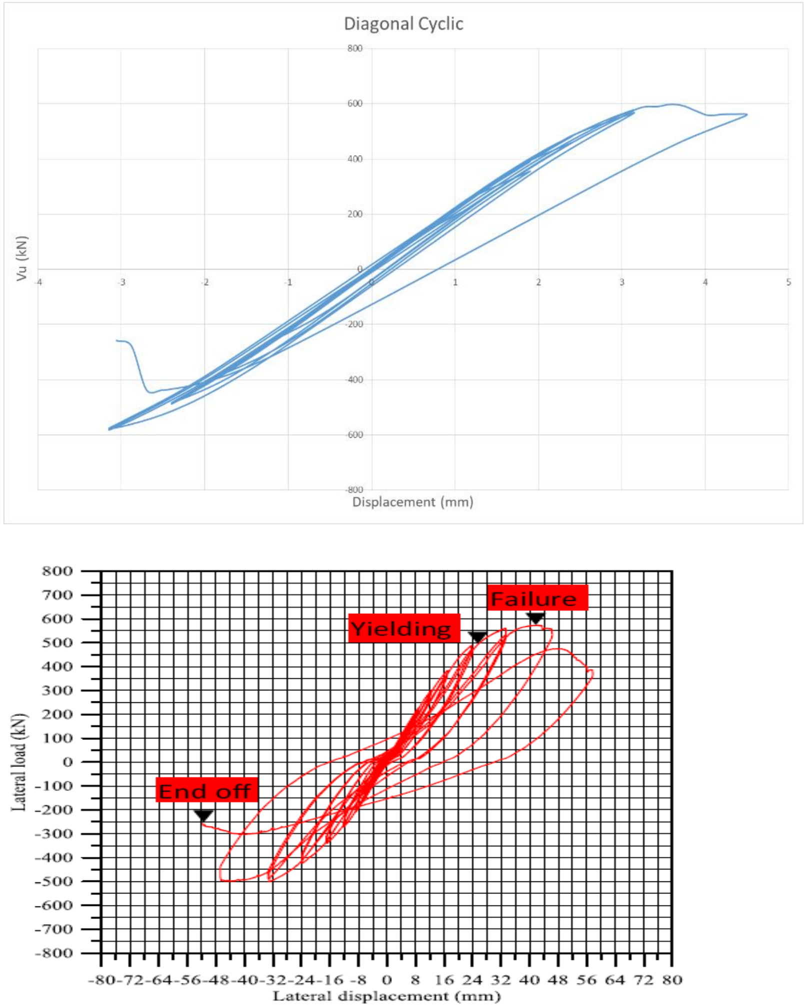

FIG.4.6: LOAD-DISPLACEMENT RELATIONSHIP OF DRCB-FC SPECIMEN.

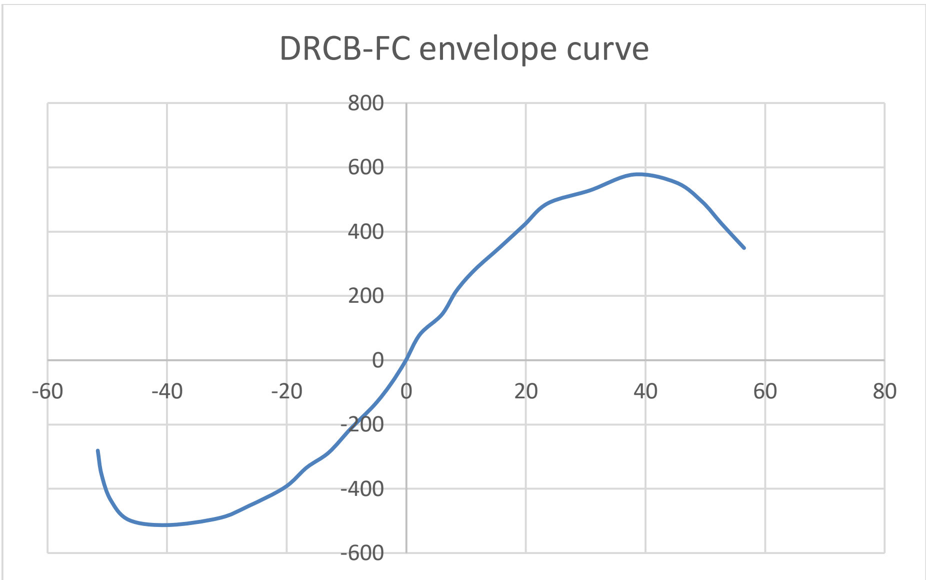

FIG.4.7 DRCB-FC ENVELOPE CURVE.

The static ductility was computed using the following equation:

$u = \frac{\partial u}{\partial y}$.

According to the observed results from Fig.4.6, the calculated ductility for the DRCB-FC specimen is 1.93. Although the DRCB-FC specimen presented a significantly higher ductility compared to the previous CRCB specimen, this ductility still falls within the low category as stated in FEMA 306. Low ductility in this DRCB-FC specimen means that this beam cannot undergo large plastic distortions before failing and it will absorb little energy before it collapses.

TABLE 4.3: DRCB-FC DUCTILITY

	∂Y	∂U	$u = \partial u / \partial y$
NUMERICAL SPECIMEN	1.88	3.63	1.93
EXPERIMENTAL SPECIMEN	1.62	3.08	1.90

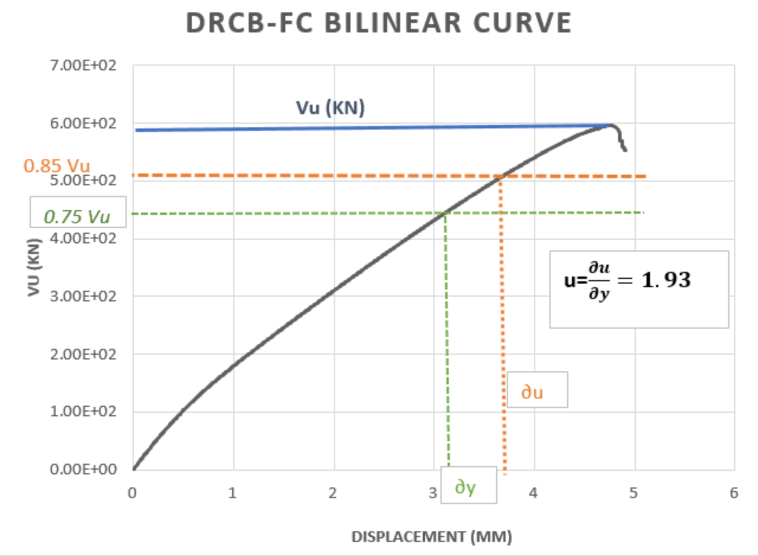

FIG.4.8: DRCB-FC BILINEAR RESPONSE CURVE.

4.5 Shear Strength Analysis

Stresses developed in the reinforcing bars are required to approximate the shear carried by reinforcing steel. Fortunately, from the above bilinear curve (see Fig.4.8), the design shear strength of the DRCB-FC can be determined. Additionally, equations from the international standard codes were used to compute shear strength. The following tables displays numerical experimental shear strength and theoretical shear strength results from the codes.

Table 4.4: Shear Strength Results for the DRCB-FC

Numerical Shear Strength	Vu = 596 KN
Experimental Shear Strength	Vu = 573 KN
Factored Shear Stress $0.33\sqrt{f'c}$.Acw	Vu=148.5 KN

TABLE 4.5: THEORETICAL SHEAR STRENGTH FOR DRCB-FC

International Standard Codes	Shear Strength
ACI 318-14	Vn = 570KN
Turkish Earthquake code 2018	Vt = 357.5 KN
RPA99/V2003	τb =222 KN
EC8	VEd = 246.27KN

The above theoretical shear strength results are well demonstrated in the following bar charts.

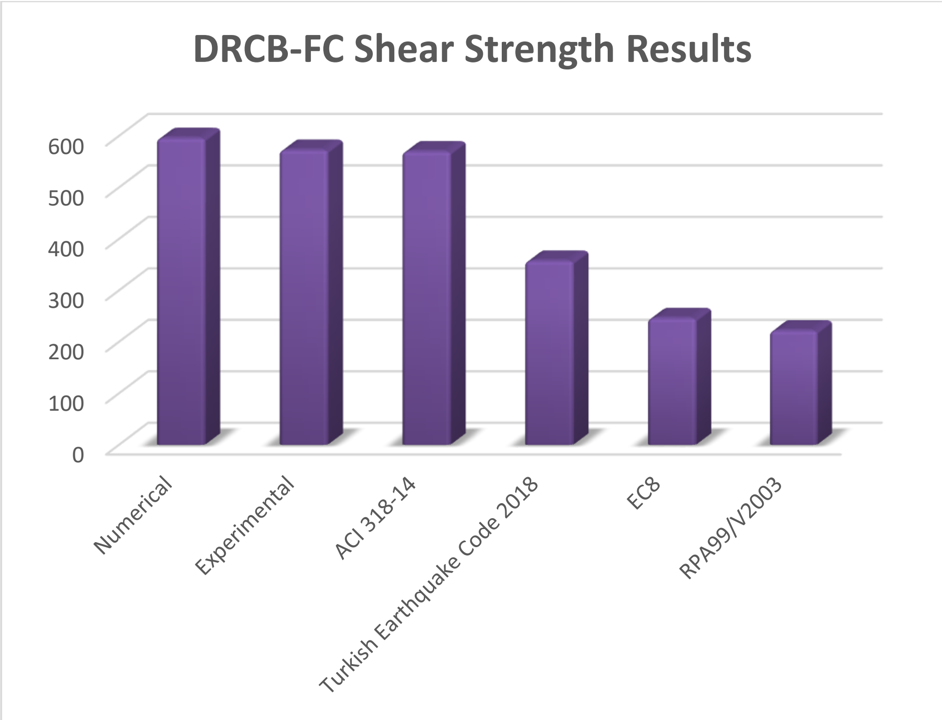

FIG.4.9: DRCB-FC SHEAR STRENGTH.

4.6 Conclusion

The nonlinear finite element executions done in Cast3m software for the DRCB-FC specimen, resulted in detailed insights of the beam's behaviour under lateral loadings. The diagonal reinforced bars on the beam' span were able to meet the high shear strength requirements compared to the CRCB. The increase in shear capacity revealed that the DRCB-FC is capable to resist flexural forces. Presence of the diagonal bars and the stirrups enhanced shear resistance capacity. However, the stirrups were predicted to fail due to buckling, the single diagonal crack proved that the DRCB-FC specimen underwent shear failure.

The following Figures reveal a summary of the test results that were observed in this study:

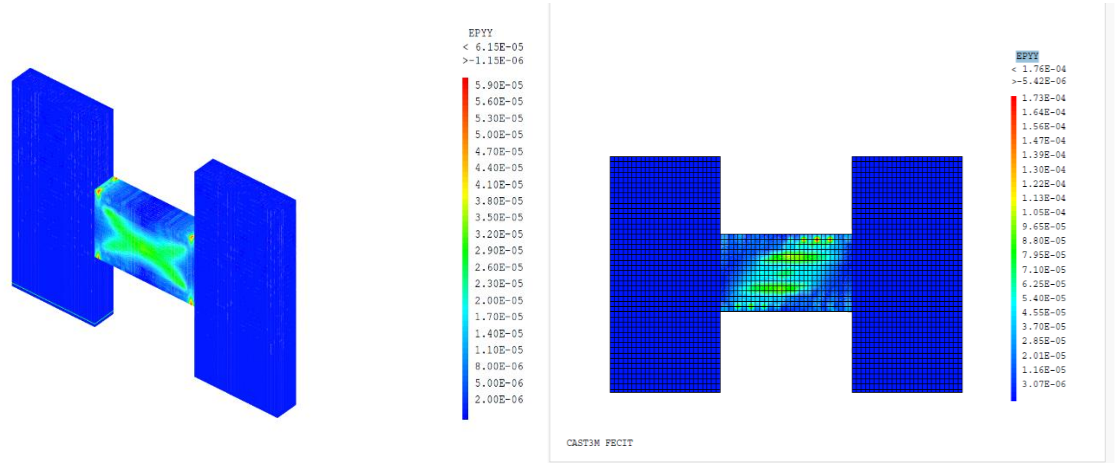

(a) (b)

FIG.5.1: (A) CRCB AND DRCB-FC UNDER QUASI-STATIC CYCLIC LOADING.

The diagonally reinforced with full confined concrete coupling beam (DRCB-FC) exhibited higher shear strength with 57.5% of the overall shear strength compared to the conventionally reinforced concrete coupling beam which had 42.5% (see Fig.5.2).

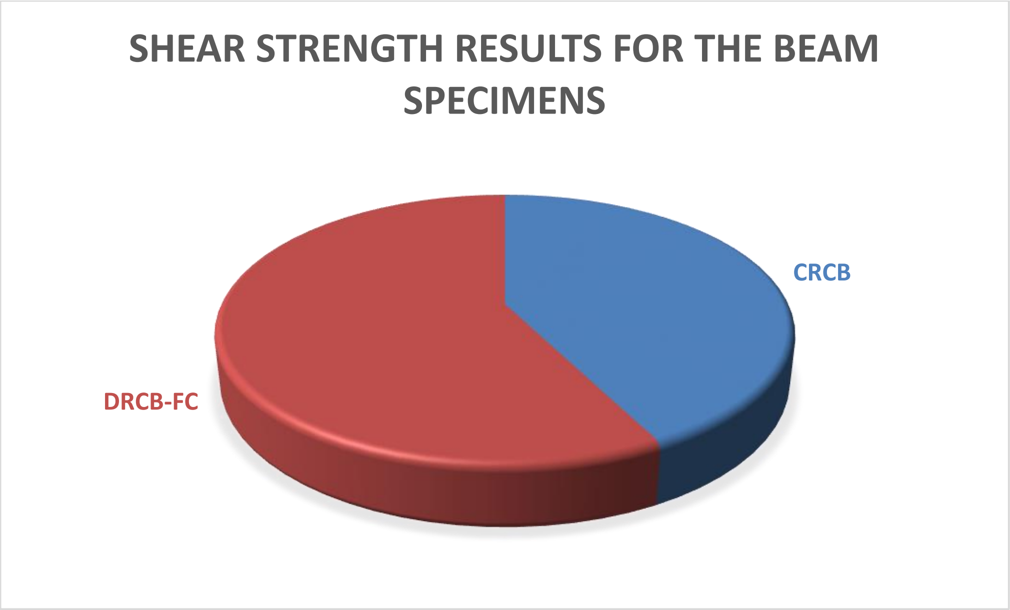

FIG.5.2: DRCB-FC AND CRCB NUMERICAL SHEAR STRENGTH RESULTS.

This explains that the DRCB-FC enhanced ductility capacity and energy dissipation capacity as compared to the CRCB; the non-linear force-displacement curves clearly illustrate this (see Fig.5.3).

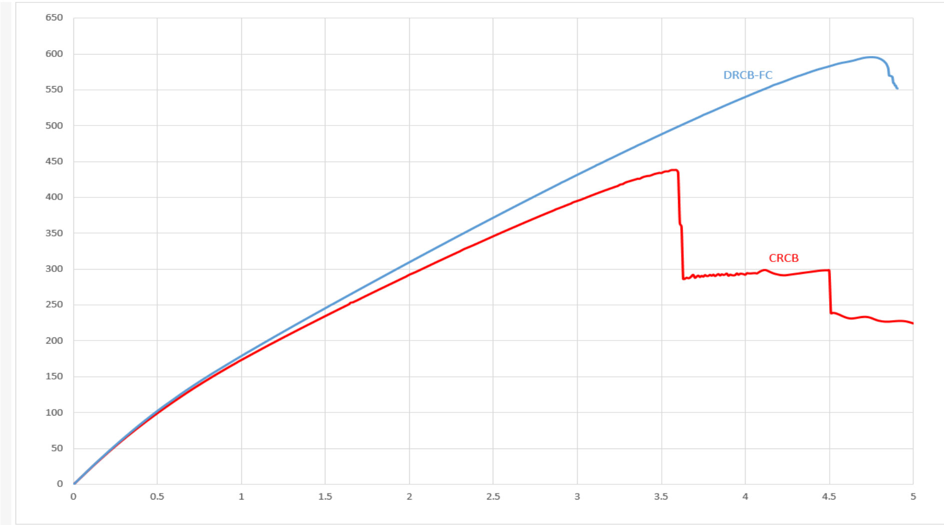

Fig.5.3 DRCB-FC and CRCB bilinear pushover curves.

The DRCB-FC specimen resulted in a greater ductility capacity as compared to the CRCB one (See Fig.5.4). A summary of the numerical and the experimental ductility results is displayed in the following figure (See Fig.55).

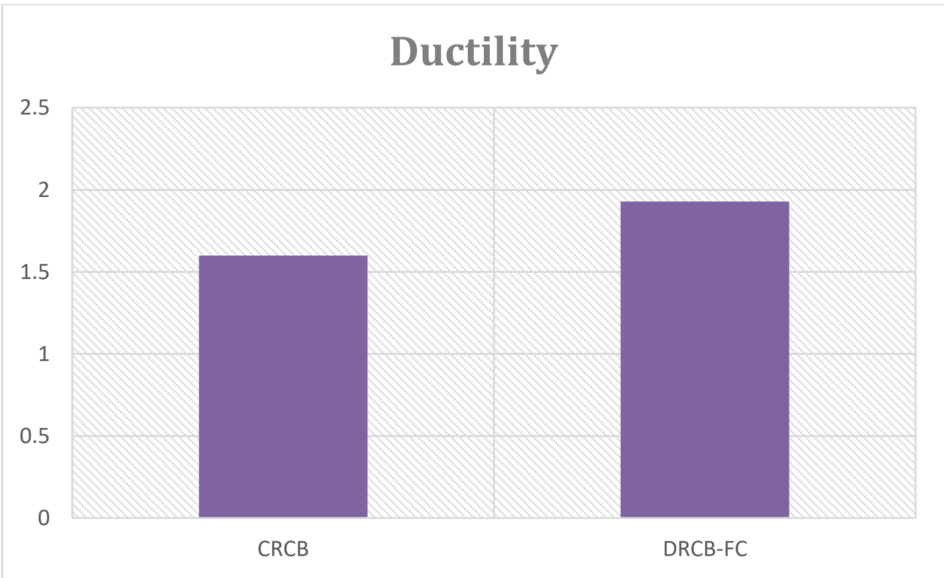

FIG.5.6: DUCTILITY RESULTS FOR CRCB AND DRCB-FC SPECIMENS.

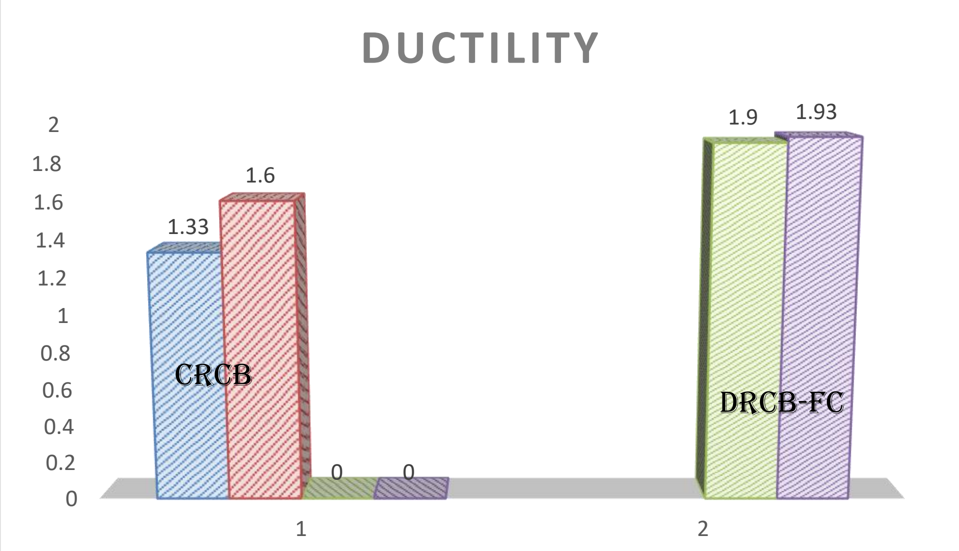

	1	2
Exp	1.33	
Num	1.6	
EXPE	0	1.9
NUME	0	1.93

FIG.5.6: NUMERICAL AND EXPERIMENTAL DUCTILITY RESULTS FOR BOTH SPECIMENS.

GENERAL CONCLUSION

General Conclusion

In this research, conventionally reinforced and diagonally reinforced (with full confined section) concrete short coupling beam specimens were simulated using Cast3m software. The specimens were modelled nonlinearly following the ACI 318-14 and the Turkish Earthquake Code 2018. Moreover, the numerical beam specimens represented the experimental specimens provided in the previous experimental study done by Hansan Sesli and Metin Husem. Our numerical test setup was done in a way only to understand the post-elastic behaviour of short coupling beams, with the exemption of the shear wall piers, which were treated elastically. Therefore, no post-elastic results were obtained for the shear walls.

Both beams evaluated in this study (CRCB and DRCB-FC) were subjected to static and quasi-static cyclic loading with an aspect ratio of two and factored shear stress of $0.33\sqrt{f'c}.Acw$. The CRCB exhibited diagonal intense tension failure with double diagonal cracks across the beam section. Whereas the DRCB-FC only showed mild single-lined diagonal crack, this was due to sufficient shear resistance reinforcements (stirrups and diagonal bars), which enhanced shear resistance.

The coupling beam specimens of this study revealed satisfactory performance in terms of life safety as per ASCE/SEI 41-17. It is predicted that the integrity of humans will be met during earthquake actions, although given a limited duration for exit. From the theoretical results provided by the International Standard Codes, the coupling beam specimens revealed a satisfactory performance in terms of shear strength.

If more specimens were tested for different aspect ratios and reinforcement configurations, more results that are satisfactory would be obtained. Further research is required to numerically and experimentally study shear wall piers in the post-elastic state, to evaluate in detail the effect of coupling beams in shear walls. Additionally, as most of the equations provided by the international standard codes are limiting, in the future, further research should be carried out, applying advanced methods to study the coupling beam’s behaviour.

REFERENCES

References

318-19 Building Code Requirements for Structural Concrete and Commentary. (2019). American Concrete Institute. https://doi.org/10.14359/51716937

Aktan, A. E., & Bertero, V. V. (1981). *The seismic resistant design of R/C coupled structural walls* (p. 17417).

Appplied Technology Council. (2007). *Federal Emergency Management Agency FEMA 461*.

Aristizabal-Ochoa, J. D. (1983). Seismic Analysis of Slender Coupled Walls. *Journal of Structural Engineering*, *109*(7), 1538–1552. https://doi.org/10.1061/(ASCE)0733-9445(1983)109:7(1538)

B. A. Canbolat, G. Parra-Montesinos, J. Wight. (2005). Experimental Study on Seismic Behavior of High-Performance Fiber-Reinforced Cement Composite Coupling Beams. *ACI Structural Journal*, *102*(1). https://doi.org/10.14359/13541

Bahaa Ahmad Burhan Al-khateeb. (2021). *Experimental study of reinforced concrete coupling beams with axial restraint*. Washington State University.

Bhunia, D., Prakash, V., & Pandey, A. D. (2013). A Conceptual Design Approach of Coupled Shear Walls. *ISRN Civil Engineering*, *2013*, 1–28. https://doi.org/10.1155/2013/161502

Breña, S. F., & Ihtiyar, O. (2011). Performance of Conventionally Reinforced Coupling Beams Subjected to Cyclic Loading. *Journal of Structural Engineering*, *137*(6), 665–676. https://doi.org/10.1061/(ASCE)ST.1943-541X.0000316

Building Code Requirements for Structural Concrete (ACI 318-14) [and] Commentary on Building Code Requirements for Structural Concrete (ACI 318R-14). (2014).

D. Naish, A. Fry, +1 author J. Wallace. (2013). Reinforced Concrete Coupling Beams—Part II: Modeling. *ACI Structural Journal*, *110*(06). https://doi.org/10.14359/51686161

Eurocode 8, design of structures for earthquake resistance. (2005). British Standards Institution.

REFERENCES

Fantilli, A. P., Mihashi, H., & Vallini, P. (2009). Multiple cracking and strain hardening in fiber-reinforced concrete under uniaxial tension. *Cement and Concrete Research*, *39*(12), 1217–1229. https://doi.org/10.1016/j.cemconres.2009.08.020

Fortney, P. J., Shahrooz, B. M., & Rassati, G. A. (2006). The Next Generation of Coupling Beams. *Composite Construction in Steel and Concrete V*, 619–630. https://doi.org/10.1061/40826(186)58

G.B Barney, K.N. Shiu, B.G.Rabbat and A.E.Fiorata. (1976). *Earthquake resistant structural walls-Tests of coupling beams*.

Gong, B., & Shahrooz, B. (2001). Steel-concrete composite coupling beams—Behavior and design. *Engineering Structures*, *23*, 1480–1490. https://doi.org/10.1016/S0141-0296(01)00042-6

Gustavo J. Parra-Montesinos. (2005). High-Performance Fiber-Reinforced Cement Composites: An Alternative for Seismic Design of Structures. *ACI Structural Journal*, *102*(5). https://doi.org/10.14359/14662

HungChung-Chan & LuWei-Ting. (2015). Towards achieving the desired seismic performance for hybrid coupled structural walls. *Earthquakes and Structures*, *9*(6), 1251–1272.

I. A. Tegos and G. Gr. Penelis. (1988). Seismic Resistance of Short Columns and Coupling Beams Reinforced With Inclined Bars. *ACI Structural Journal*, *85*(1). https://doi.org/10.14359/2992

Jang, S.-K., & Hong, S.-G. (n.d.). *THE SHEAR STRENGTH OF RC COUPLING BEAMS WITH PLASTIC HINGES USING STRUT-AND-TIE MODEL*.

Kaufmann et al.,2020. (2020). *IDEA STATICA DETAIL 20-The theoretical background is based on stress field design of structural concrete*.

Kwan, A. K. H., & Zhao, Z.-Z. (2002). Cyclic behaviour of deep reinforced concrete coupling beams. *Proceedings of the Institution of Civil Engineers - Structures and Buildings*, *152*(3), 283–293. https://doi.org/10.1680/stbu.2002.152.3.283

REFERENCES

Lim, E., Hwang, S.-J., Wang, T.-W., & Chang, Y.-H. (2016). An Investigation on the Seismic Behavior of Deep Reinforced Concrete Coupling Beams. *ACI Structural Journal*, *113*(2). https://doi.org/10.14359/51687939

Luciano Galano and Andrea Vignoli. (2000). Seismic Behavior of Short Coupling Beams with Different Reinforcement Layouts. *ACI Structural Journal*, *97*(6). https://doi.org/10.14359/9633

Macdonald, A. J. (1997). *Structural design for architecture* (1. publ). Architectural Press.

Mata Falcón, J., Weber, M., & Kaufmann, W. (2022). *Application of compatibility-based stress fields for the quantification of minimum shear reinforcement: Aplicación de campos de tensiones considerando compatibilidad de deformaciones para la cuantificación de la armadura mínima de cortante* [Application/pdf]. 10 p. https://doi.org/10.3929/ETHZ-B-000554282

MINISTERE DE L'HABITAT (RPA99/Version20030. (n.d.). *Centre National de recherche applique en Genie-parasismique*, 121.

Monthian Setkit. (2012). *Seismic behavior of slender coupling beams construted with high performance fiber-reinforced concrete*. The University of Michigan.

Navrátil, J., Ševčík, P., Michalčík, L., Foltyn, P., & Kabeláč, J. (2017). *A SOLUTION FOR WALLS AND DETAILS OF CONCRETE STRUCTURES*.

Paulay, T., and Binney, J. R. (2011). Diagonally Reinforced Coupling Beams of Shear Walls. *318Reference*, *21*(52).

R.Park and T.Paulay. (1974). *Reinforced Concrete Structures* (Wiley-interscience publication). John Wiley and sons.

Santhakumar, A. R. (n.d.). *Ductility of coupled shear walls*.

Schlaich, J., Schafer, K., & Jennewein, M. (1987). Toward a Consistent Design of Structural Concrete. *PCI Journal*, *32*(3), 74–150. https://doi.org/10.15554/pcij.05011987.74.150

REFERENCES

Seismic evaluation and retrofit of existing buildings: ASCE/SEI, 41-17. (2017). American Society of Civil Engineers.

Sesli, H., & Husem, M. (2021). Experimental Investigation on Cyclic Behavior of Reinforced Concrete Coupling Beams Under Quasi-static Loading. *International Journal of Civil Engineering*, *19*(4), 381–400. https://doi.org/10.1007/s40999-020-00573-w

T. Tassios, M. Moretti, A. Bezas. (1996). On the Behavior and Ductility of Reinforced Concrete Coupling Beams of Shear Walls. *ACI Structural Journal*, *93*(6). https://doi.org/10.14359/518

Takale, A. B., & Taware, A. A. (2023). *Study of the Seismic Behavior of Diagonally Reinforced Concrete Coupling Beam with Compared to Composite Beam* [Preprint]. In Review. https://doi.org/10.21203/rs.3.rs-3152096/v1

T.Paulay. (1969). *The coupling of shear walls*. University of Canterbury Christchurch New Zealand.

Yan Xiao, Asadollah Esmaeily-Ghasemabadi, and Hui Wu. (1999). High-Strength Concrete Short Beams Subjected to Cyclic Shear. *ACI Structural Journal*, *96*(3). https://doi.org/10.14359/673